**A Volcano Rekindled: The Renewed Eruption of Mount St. Helens, 2004–2006**
Edited by David R. Sherrod, William E. Scott, and Peter H. Stauffer
U.S. Geological Survey Professional Paper 1750, 2008

# Chapter 2

# Seismicity Associated with Renewed Dome Building at Mount St. Helens, 2004–2005

By Seth C. Moran[1], Stephen D. Malone[2], Anthony I. Qamar[2*], Weston A. Thelen[2], Amy K. Wright[2], and Jacqueline Caplan-Auerbach[3]

## Abstract

The reawakening of Mount St. Helens after 17 years and 11 months of slumber was heralded by a swarm of shallow (depth <2 km) volcano-tectonic earthquakes on September 23, 2004. After an initial decline on September 25, seismicity rapidly intensified; by September 29, $M_d$ >2 earthquakes were occurring at a rate of ~1 per minute. A gradual transition from volcano-tectonic to hybrid and low-frequency events occurred along with this intensification, a characteristic of many precursory swarms at Mount St. Helens before dome-building eruptions in the 1980s. The first explosion occurred October 1, 2004, 8.5 days after the first earthquakes, and was followed by three other explosions over the next four days. Seismicity declined after each explosion and after two energetic nonerruptive tremor episodes on October 2 and 3. Following the last explosion of this series, on October 5, seismicity declined significantly. Over the next ten days seismicity was dominated by several event families; by October 16, spacing between events had become so regular that we dubbed the earthquakes "drumbeats." Through the end of 2005 seismicity was dominated by these drumbeats, although occasional larger earthquakes ($M_d$ 2.0–3.4) dominated seismic energy release. Over time there were significant variations in drumbeat size, spacing, and spectra that correlated with changes in the style of extrusion at the surface. Changes in drumbeat character did not correspond to variations in magma flux at the conduit, indicating that drumbeat size and spacing may be more a function of the mechanics of extrusion than of the extrusion rate.

[1] U.S. Geological Survey, 1300 SE Cardinal Court, Vancouver, WA 98683

[2] Pacific Northwest Seismic Network, Department of Earth and Space Sciences, University of Washington, Box 351310, Seattle, WA 98195

[3] Geology Department, Western Washington University, 516 High Street, Bellingham, WA 98225

* Deceased

## Introduction

As of the writing of this paper (2006), more than 26 years of recorded seismic history have accumulated at Mount St. Helens since the Pacific Northwest Seismic Network's (PNSN) digital recording system began operation in March 1980. This 26-year period includes the precursory buildup to the May 18, 1980, eruption (Endo and others, 1981; Malone and others, 1981), post-May 18, 1980, seismicity associated with the 20 eruptions occurring between 1980 and 1986 (Malone, 1983; Malone and others, 1983; Swanson and others, 1985; Swanson and Holcomb, 1990), quiescence between 1987 and 2004 (Moran, 1994; Musumeci and others, 2002), and the onset of the eruption in 2004. This history is made all the richer by its being recorded on a relatively dense seismic network of short-period vertical-component seismometers in place since shortly after the first earthquakes began in late March of 1980 (fig. 1). Seismic data recorded by this network have been used in many studies, including (1) forecasting eruptions and detecting explosions (Endo and others, 1981; Malone and others, 1981; Malone and others, 1983; Swanson and others, 1983; Endo and others, 1990; Jonientz-Trisler and others, 1994); (2) eruption dynamics (Qamar and others, 1983; Weaver and others, 1983; Shemeta and Weaver, 1986); (3) modeling the Mount St. Helens magmatic system (Weaver and others, 1981; Scandone and Malone, 1985; Endo and others, 1990; Barker and Malone, 1991; Moran, 1994; Musumeci and others, 2002); (4) interpreting the structure of the magmatic system through tomography (Lees and Crosson, 1989; Lees, 1992; Moran and others, 1999), earthquake locations (Fehler, 1985; Weaver and others, 1987; Musumeci and others, 2002), and *b* values (Endo and others, 1981; Wiemer and McNutt, 1997); (5) determining the source process responsible for various type of seismic signals recorded at Mount St. Helens (Fehler and Chouet, 1982; Malone, 1983; Fehler, 1985; Norris, 1994); (6) describing the stress field associated with the magmatic system (Barker and Malone, 1991; Moran, 1994;

Giampiccolo and others, 1999; Musumeci and others, 2002); and (7) defining repetitive events (or earthquake families), including the first published study of repetitive events in a volcanic setting (Frémont and Malone, 1987).

As a result of these and other studies, by 2004 we had a fairly good working model of the magmatic system beneath Mount St. Helens. We also had a very good understanding of the character of typical eruptive and noneruptive seismicity. These perspectives proved vital to our ability to correctly assess the significance of seismicity when Mount St. Helens reawakened in 2004.

The reawakening of Mount St. Helens was heralded by a swarm of shallow (depth <2 km) volcano-tectonic (VT) earthquakes beginning at roughly 0200 Pacific daylight time (PDT) on September 23, 2004. More than one million earthquakes were recorded by the end of 2005, with events occurring every 1 to 5 minutes. Of these, roughly 8,000 events were located by the PNSN through the end of 2005. Many will likely never be located, even with sophisticated crosscorrelation and relative relocation techniques (for example, Thelen and others, this volume, chap. 4), because many are small, occur in the coda of previous events, and (or) have nonimpulsive arrivals. With such a sizable dataset we are still very much in discovery mode, and it is likely that at least some of what we present in this paper will be superseded by subsequent research. Our principal purpose is to give an overview of our understanding of seismicity that occurred before and during the eruption in 2004–5, as well as to put the eruption's seismicity in the broader context of the 26 years of seismic history of Mount St. Helens.

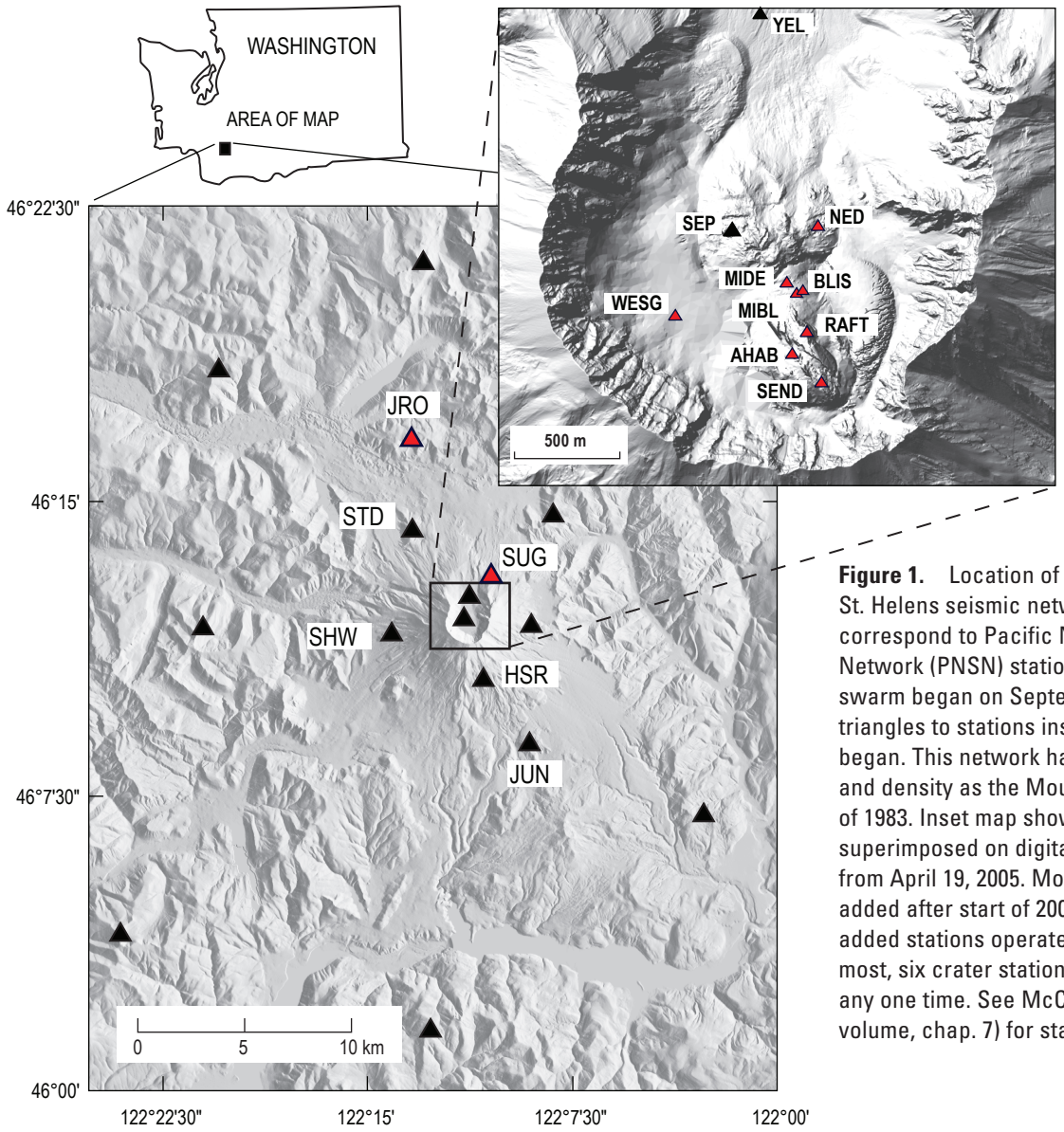


**Figure 1.** Location of stations in Mount St. Helens seismic network. Black triangles correspond to Pacific Northwest Seismic Network (PNSN) stations in place when swarm began on September 23, 2004, and red triangles to stations installed after eruption began. This network had similar geometry and density as the Mount St. Helens network of 1983. Inset map shows crater stations superimposed on digital elevation model from April 19, 2005. Most crater stations were added after start of 2004 eruption. Many newly added stations operated for short periods; at most, six crater stations were operational at any one time. See McChesney and others (this volume, chap. 7) for station installation details.

## Seismicity During Quiescence, 1987–2004

Although short-term precursory seismicity began on September 23, 2004, in a longer term view the first precursory seismicity likely started as early as late 1987 (fig. 2), when the first of several years-long swarms of "deep" (>3 km) VT events began (Moran, 1994). The depth of these swarms contrasted sharply with the exclusively shallow (<3 km) precursory swarms associated with 19 of the 20 post-May 18, 1980, dome-building eruptions (Malone and others, 1983). In map view, the deeper events were concentrated to the north and south of the 1980–86 lava dome (Moran, 1994; Musumeci and others, 2002), in contrast to the east-west orientation of "deep" VT events that extended to 20 km immediately after the May 18, 1980, eruption (Weaver and others, 1981; Shemeta and Weaver, 1986; Barker and Malone, 1991; Moran, 1994). Fault-plane solutions for the post-May 18, 1980, "deep" events had tangentially oriented P axes with respect to the 1980 crater, in contrast to radially oriented P axes for post-1987 "deep" events (Barker and Malone, 1991; Moran, 1994; Musumeci and others, 2002). The changes in stress-field orientation and epicentral distribution are best explained by a pressure decrease in the magmatic plumbing system after 1980 and a pressure increase after 1986 (Barker and Malone, 1991; Moran, 1994; Musumeci and others, 2002). Moran (1994) argued that sizable swarms preceding the last two dome-building eruptions in 1986 were an indication of the formation of a plug in the conduit to the surface, a plug that subsequent batches of magma were unable to penetrate. The occurrence of six phreatic explosions in 1989–91 (Mastin, 1994) and detection of magmatic $CO_2$ in association with the last significant months-long swarm of deeper seismicity in 1998 (Gerlach and others, this volume, chap. 26) provide further evidence that intrusion of magma may have occurred between 1987 and 2004.

Most seismicity after 1998 was concentrated at depths ~2 km below the crater floor, although occasional deeper and shallower VT events also occurred (fig. 2). The 2-km-deep seismicity band could represent the development of a fracture system in the base of the plug inferred by Pallister and others (1992) and Moran (1994) to extend from the surface down to 2 km. The *b* values for earthquakes in this depth range increased marginally from 0.8–1.0 before 1992 to 1.0–1.4 after 1992 (fig. 3). The *b* values for events between 3 and 10 km showed no such change over the same time period, indicating that the shallow *b*-value change is not a result of a systematic bias in the PNSN catalog. The *b*-value increase, if real, could indicate an increase in the number of small fractures (Mogi, 1962) between 1991 and 1993 and is the type of change that would be expected in association with the

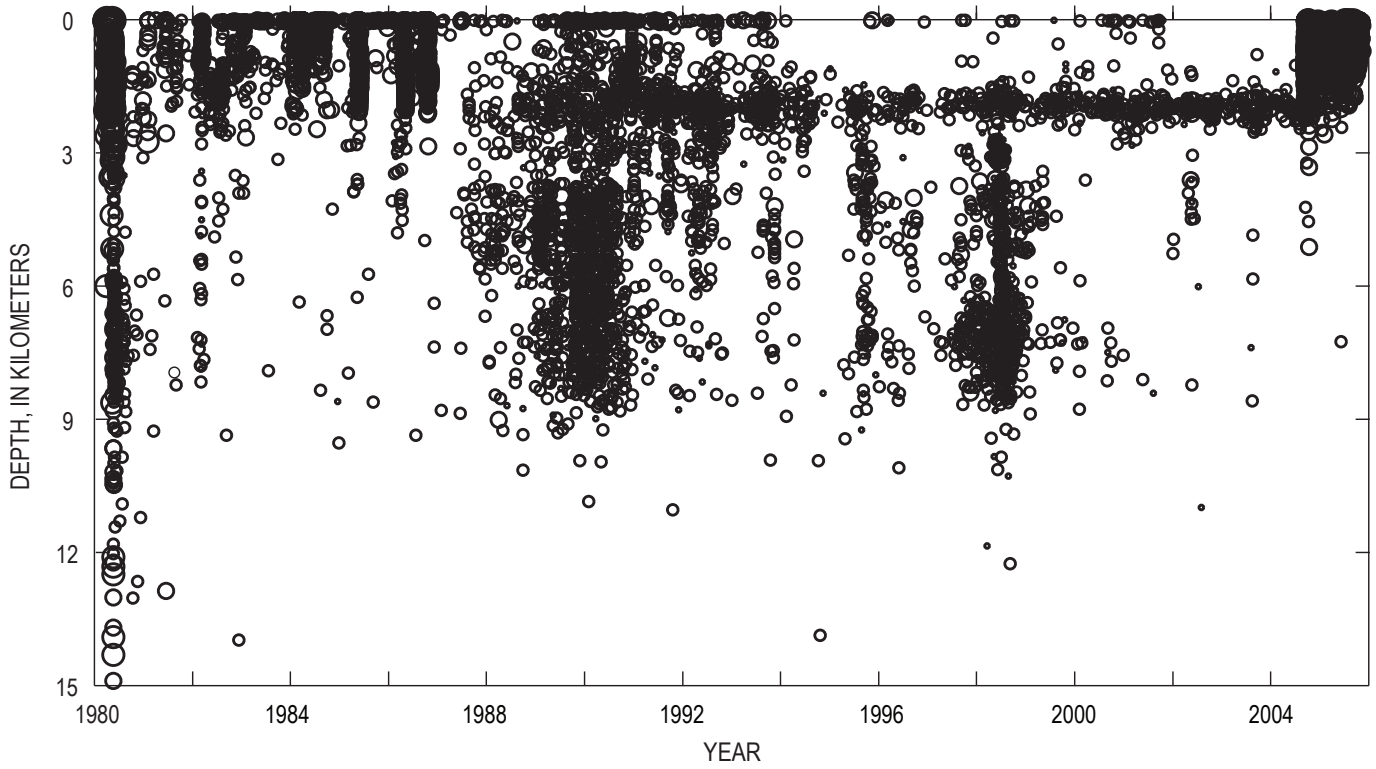


**Figure 2.** Time versus depth plot showing all earthquakes (circles) with well-constrained locations (gap <135°, nearest station <2 km, and arrival times on at least seven stations) occurring at Mount St. Helens between 1980 and 2005. Depths are relative to a datum corresponding to average altitude of stations in Mount St. Helens network, roughly 1.1 km above sea level. Horizontal-axis tick marks indicate start of a year, with gaps of 2 years between tick marks.

fracturing of the base of a plug (Vinciguerra and others, 2001). However, *b* values remained relatively constant in the subsequent 12 years leading up to the 2004 eruption (fig. 3), despite the evidence for a possible intrusion of magma in 1998.

The last significant earthquake swarm of the 1987–2004 quiescent period occurred on November 2–4, 2001. The swarm began relatively abruptly at around 1730 Pacific standard time (PST) on November 2 and consisted of many small (most with coda-duration magnitudes $M_d$ <0.0, with the largest $M_d$ 1.8) and shallow (<2 km) VT events occurring at a rate of 2–3 per minute. There were also a number of 10–30-minute-long spasmodic bursts of 8–10 VT events per minute. The Cascades Volcano Observatory (CVO) issued an Information Statement at 1800 PST on November 3, 2001, stating that a swarm was underway with no evidence that an eruption was imminent. Following the last spasmodic burst of VTs at 0400 PST on November 4, the number and size of earthquakes declined steadily, reaching background levels by November 5, 2001.

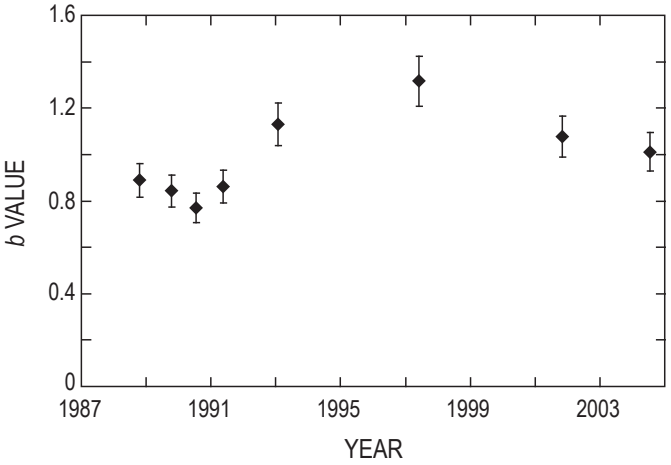


**Figure 3.** Plot of *b* values for shallow (depths <3 km) earthquakes occurring between 1987 and 09/23/2004, the last day for which the PNSN catalog is complete. Horizontal-axis tick marks indicate start of a year, with gaps of 2 years between tick marks. The *b* values are computed using maximum-likelihood method (Bender, 1983) and are determined for nonoverlapping groups of 150 events with $M_d$ 0.4 (magnitude of completeness for entire interval) selected with same criteria used for earthquakes shown in figure 2.

# September 23–October 5, 2004: Vent-Clearing Phase

## September 23–September 25, 2004

The first short-term signs of unrest came in the form of a swarm of VT events starting at roughly 0200 PDT on September 23, 2004 (fig. 4), with the onset of unrest defined as the time when hourly event counts reached sustained levels above 1–2 events per hour. The number of earthquakes increased throughout September 23, peaked midday on September 24, and then declined to a minimum early on September 25, roughly 48 hours after the swarm began. By September 24, earthquakes had become so numerous that the PNSN began locating only a subset of them, and real-time seismic amplitude measurement (or RSAM; Endo and Murray, 1991), "webicorder," and spectrogram plots became the principal tools for tracking seismicity (Qamar and others, this volume, chap. 3). All located events were shallow (<2 km) and small, with the largest a $M_d$ 2.2 and most having magnitudes <1.0. The *b* values for catalog locations were ~1, consistent with *b* values before 2004 (fig. 3). Fault-plane solutions from the PNSN catalog show a variety of failure mechanisms and stress-field orientations, with no clear dominant fracture pattern (appendix 1). To this point, seismicity closely resembled the swarm of November 2–4, 2001. This similarity governed initial interpretations by the PNSN and CVO. Although somewhat more energetic than the 2001 swarm, we judged that this swarm was within the bounds of noneruptive seismicity seen during the previous 18 years at Mount St. Helens. An information statement was released on September 24, stating that a seismic swarm was occurring at Mount St. Helens, with no indications that an eruption was imminent (Dzurisin and others, 2005; Scott and others, this volume, chap. 1).

## September 25–October 1, 2004

Seismicity departed from the 2001 script midday on September 25, 2004. Instead of continuing to decline, the earthquake rate stabilized and then began to increase (fig. 5). Lower-frequency events, including hybrid and low-frequency (LF) events (previously identified as type "m" and "l" events at Mount St. Helens in the 1980s by Malone, 1983, and Malone and others, 1983) also began occurring alongside the VT events (fig. 6). We elected to refer to these as low-frequency, or "LF," events rather than the commonly used long-period, or "LP," event label, because the definition of an LP event includes a specific source mechanism (that is, the vibration of fluid- or gas-filled cracks; Lahr and others, 1994; Chouet, 1996). Experience with low-frequency events at Mount St. Helens in the 1980s indicated that other source mechanisms might be involved, and so we felt it best to use the purely descriptive "LF event" terminology without presuming a source mechanism. It should be noted that LF events commonly have extended codas at Mount St. Helens, resulting in overly large coda-duration magnitudes relative to amplitude-based magnitudes (Qamar and others, this volume, chap. 3).

The transition from VT to hybrid and LF events took place over several days, as illustrated by the earthquake spectral amplitude (or "ESAM") plot in figure 5 (see appendix 2 for details), with LF events becoming progressively more dominant through October 5. Similar transitions in earthquake types were seen in precursory swarms preceding many dome-building eruptions at Mount St. Helens in the 1980s (Malone,

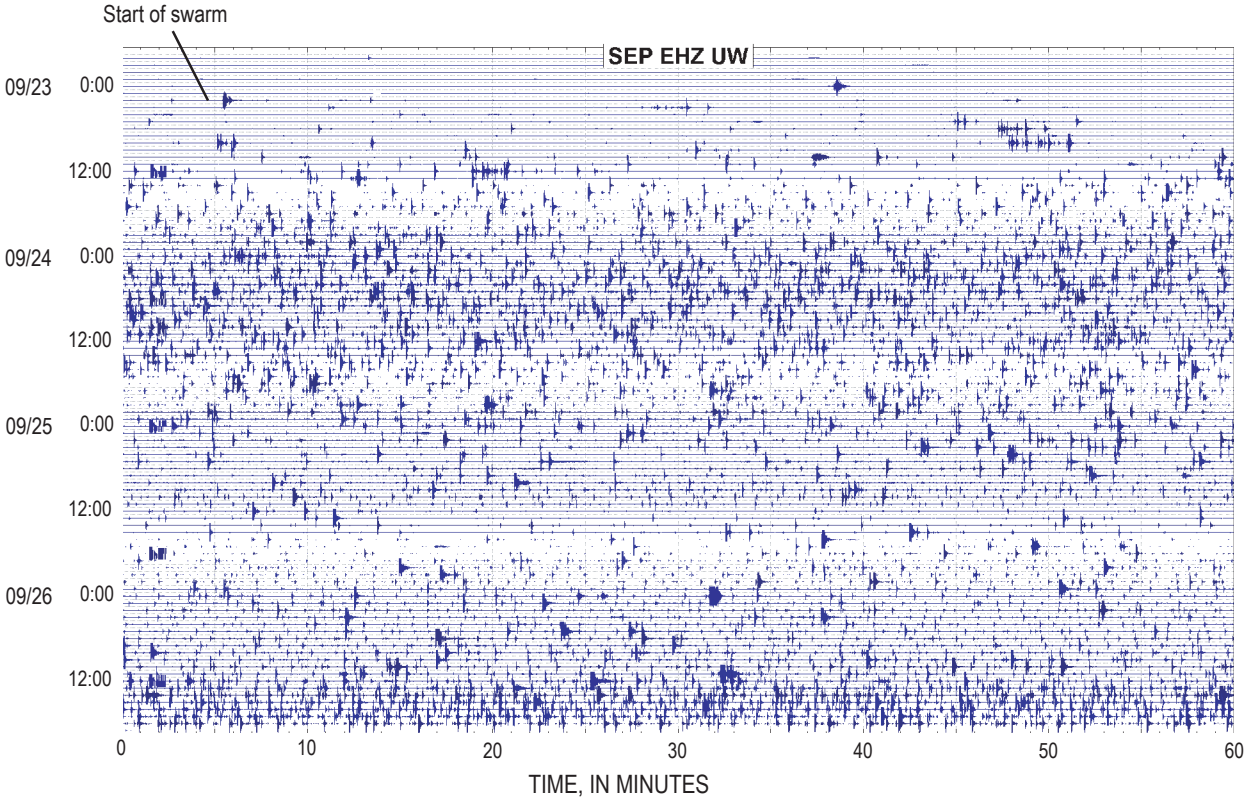


**Figure 4.** Seismic record from station SEP (~500 m north of the vent; see fig. 1) from 1900 PDT September 22 through 1900 PDT September 26, 2004, showing start of seismic swarm at 0200 PDT September 23 and buildup over next three days.

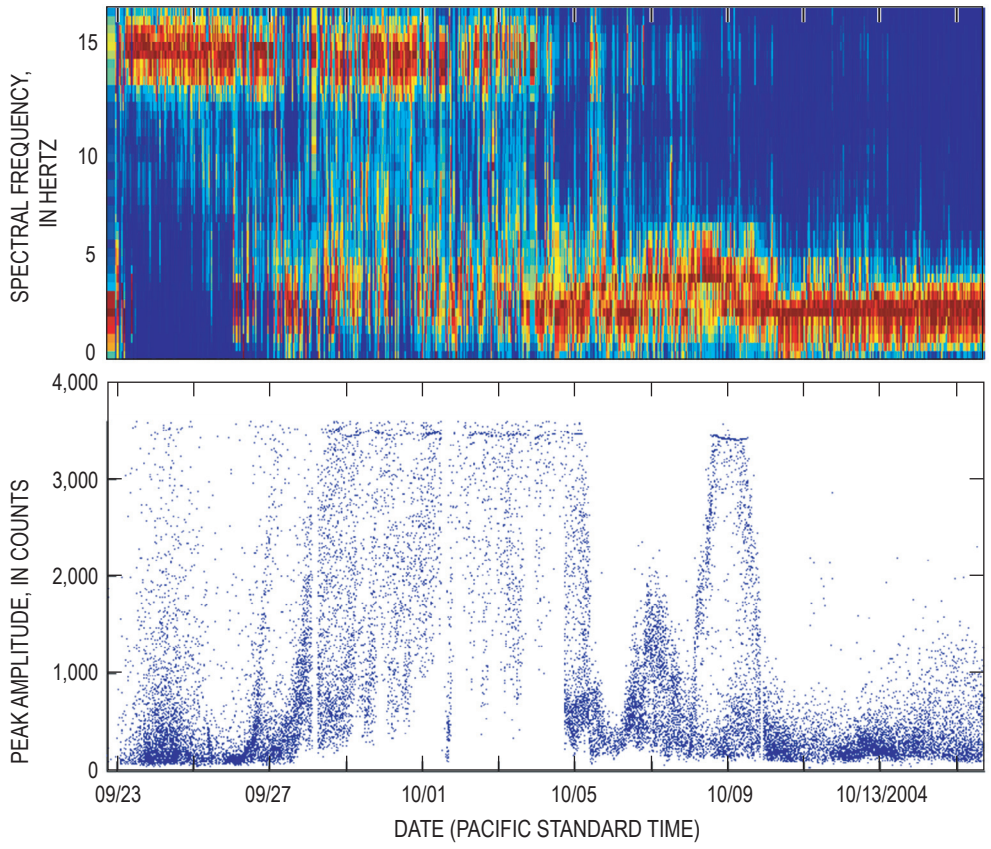


**Figure 5.** Plot of earthquake spectral amplitudes, or ESAM (top), and peak amplitudes (bottom) for detected events at station HSR (fig. 1) between September 23 and October 15, 2004 (see appendix 2 for event detection details). Horizontal-axis tick marks indicate start of a day, with gaps of 2 days between tick marks. Note that peak amplitudes clip at ~3,400 counts for station HSR.

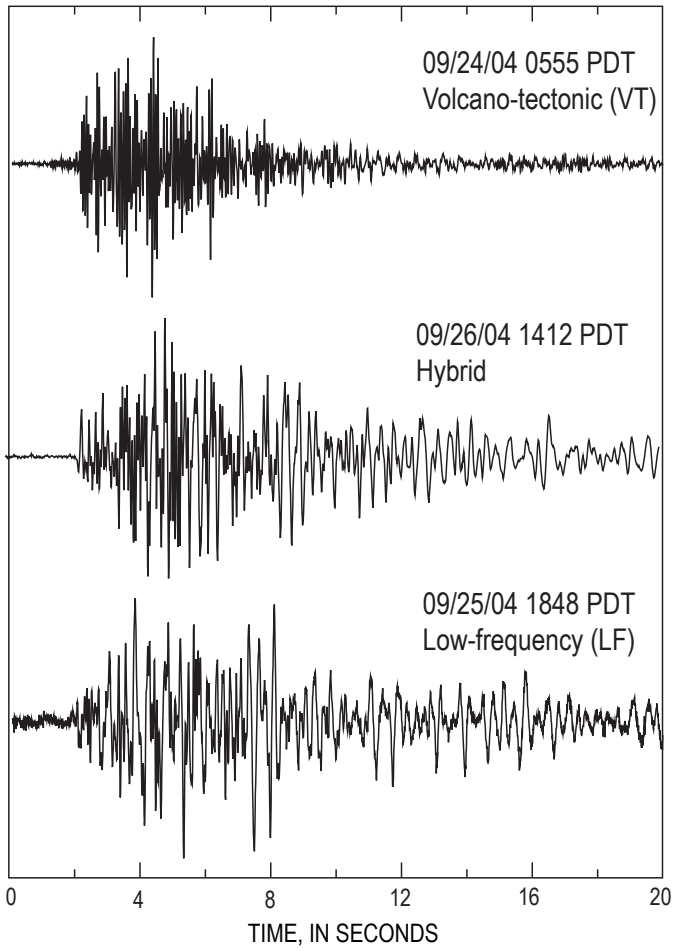


**Figure 6.** Waveforms for typical volcano-tectonic (VT), hybrid, and low-frequency (LF) events recorded at station HSR (fig. 1) during September 23–26, 2004.

1983; Malone and others, 1983), as well as in the first week of seismicity prior to the May 18, 1980, eruption (Malone and others, 1981; Endo and others, 1981). Those transitions were also gradual, taking place over periods of hours to days. The transitions before the 1980–86 dome-building eruptions were particularly noticeable several hours before eruptions commenced, and they therefore became one of the diagnostic tools that allowed for increasingly precise predictions of eruption onset times (Malone and others, 1983; Swanson and others, 1983; Swanson and others, 1985). Such changes in event character were inferred by Malone and others (1983) to represent a shallowing of the deformation front (as suggested by slightly shallower depths for type "l" events) and to be caused either by the fracturing of different rock types or by a change in source mechanism. In this context, the appearance of lower-frequency events on September 25, 2004, increased the likelihood in our minds that the seismic swarm would ultimately lead to an eruption.

By the morning of September 26 the earthquake rate had further intensified. By midday, maximum event sizes had also started increasing (fig. 5). The increase in event rate and event size and the change in event character caused CVO to issue a Notice of Volcanic Unrest (or Alert Level 1) in the afternoon of September 26. Earthquake locations showed no obvious temporal changes between September 25 and 26, in large part because station density within the crater and the velocity model were insufficient to locate shallow earthquakes in a geologically complex medium with a precision of less than several hundred meters. Between September 25 and 27, however, P-wave arrival-time differences increased between station SEP (fig. 1), located on the 1980–86 lava dome essentially on top of most earthquakes, and other stations located within 4 km of the vent (fig. 7). Daily average arrival-time differences between stations SEP and YEL increased the most (0.13 s), with differences at other stations increasing by 0.07–0.1 s. Arrival-time differences between station pairs not including SEP did not change significantly. We reexamined P-arrival picks and found no evidence that the changes in arrival-time differences were a result of analyst bias (multiple PNSN analysts were involved in picking earthquakes; Qamar and others, this volume, chap. 3) or decreased P-arrival impulsiveness at distant stations (which could result in late picks). The observed pattern is best explained by either a decrease in seismic velocity near station SEP or a decrease in earthquake depths below SEP. Although injection of magma and associated fracturing of country rock could result in lower velocities, shallowing of hypocenters is the simplest explanation for the increase in P-wave arrival-time differences. This shallowing is in part supported by the appearance on September 26 of cracks in the crater glacier (Dzurisin and others, 2005; Scott and others, this volume, chap. 1; Walder and others, this volume, chap. 13).

At roughly 1600 PDT on September 26, a series of earthquakes with similar waveforms (an earthquake "family" or multiplet; for example, see Frémont and Malone, 1987) began, at first mixed with other events with different waveforms (Thelen and others, this volume, chap. 4). By early morning of September 27, seismicity was dominated by this family, with magnitudes increasing through midday and reaching a maximum of $M_d$ 1.9 by late afternoon. This was the first clear instance of repetitive earthquakes, something that was seen frequently before dome-building eruptions at Mount St. Helens in the 1980s (Frémont and Malone, 1987) and has also been observed during other dome-building eruptions, including Usu volcano[4] in Japan (Okada and others, 1981), Augustine Volcano (Power, 1988) and Redoubt Volcano (Power and others, 1994) in Alaska, Guagua Pichincha in Ecuador (Villagómez, 2000), Soufrière Hills volcano in Montserrat (Rowe and others, 2004), and Galeras Volcano in Columbia (R. White, oral commun., 2006). Preliminary fault-plane solutions for the larger events in this family have reverse-faulting

[4] Capitalization of "Volcano" indicates adoption of the word as part of the formal geographic name by the host country, as listed in the Geographic Names Information System, a database maintained by the U.S. Board on Geographic Names. Noncapitalized "volcano" is applied informally—eds.

mechanisms, in contrast to the mix of mechanisms generated during September 23–25 (appendix 1). By 1500 on September 27, the family had become less dominant, but similar events continued through September 28.

The event rate increased relatively rapidly, to 1 event per minute, around 1700 PDT on September 27, as smaller events began occurring between the larger earthquakes (fig. 8). The size of the larger earthquakes also increased, with maximum magnitudes reaching $M_d$ 2.0–2.4 by midday on September 28. Most fault-plane solutions were dip-slip with a steeply dipping fault plane, in contrast to the reverse-faulting mechanisms dominant during the previous 24 hours (appendix 1). At this point, clipping of near-field (<4 km) stations occurred frequently. As a result, smaller events were frequently overwhelmed by the codas of the larger events, making it difficult to distinguish many individual events. It also became increasingly difficult to manually pick earthquakes and determine accurate coda magnitudes, because the coda from one event would be obscured by the onset of the next event. At this point, RSAM became the principal tool for monitoring seismicity (fig. 9), along with helicorder records from stations increasingly distant from Mount St. Helens.

Earthquakes further intensified between 0500 and 0800 on September 29 (fig. 8), when event rates increased to ~3 earthquakes per minute and maximum magnitudes rose to $M_d$ 2.4–2.8, causing CVO to issue a Volcano Advisory (or Alert Level 2) at 1040 PST (Dzurisin and others, 2005). A second rise in RSAM levels occurred 12 hours later, between 1700 and 2100 (fig. 9), when maximum magnitudes increased to $M_d$ 2.8–3.3, with $M_d$ >2 events occurring at a rate of ~1 per minute by the evening of September 29. Most fault-plane solutions for these events had normal-faulting mechanisms, although there were also occasional events with many, or all, down first-motions, consistent with reverse faulting (appendix 1). One side effect of the high rate of larger earthquakes was that they began to dominate seismic recordings at other Cascade volcano seismic networks (in particular at Mount Adams, Mount Hood, Mount Rainier, and Three Sisters), as well as at regional seismic stations in Washington and Oregon, resulting in a temporary reduction in PNSN sensitivity to smaller events in a broad area around Mount St. Helens.

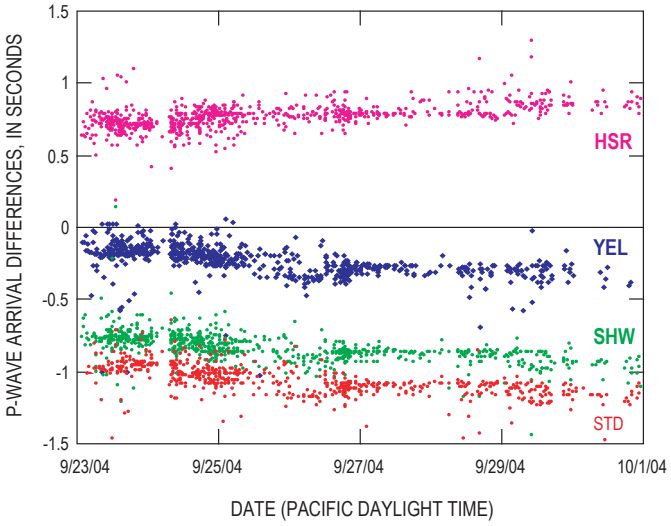


**Figure 7.** Plot of P-wave arrival-time differences between station SEP (located on the 1980–86 lava dome) and four other stations including HSR (magenta), YEL (dark blue), SHW (green), and STD (red), between September 23 and October 1, 2004. (see fig. 1 for station location). P-wave arrival-time differences were computed only for high-quality picks, with an estimated picking error of ≤0.05 s. Note that the absolute value of differences increases on all station pairs between September 25 and September 27. This increase was not apparent on other non-SEP station pairs and is consistent with shallowing of hypocenters.

Following the second intensification on September 29, the rate of larger earthquakes declined somewhat, resulting in a decline in RSAM values, which reached a relative minimum at roughly 0500 on September 30 (fig. 9). The rate of larger earthquakes increased and decreased two more times on September 30, with RSAM values always between the minimum and maximum levels achieved on September 29. The increases did not correspond with any known changes in the crater, although temporal resolution of visual observations and measurements from other geophysical instrumentation were insufficient to detect changes on an hourly scale. Fault-plane solutions from the PNSN catalog switched from dominantly normal-faulting to reverse-faulting solutions for a short time between 2300 September 30 and 0500 October 1 (appendix 1); then, three hours later at 0800, RSAM levels again increased as a result of an increase in event rate (figs. 8, 9). RSAM values peaked at 1100 at levels similar to previous maxima. The first phreatic explosion occurred an hour later at 1202 PDT, 8.5 days after the first precursory seismicity on September 23. This interval was one day longer than the 7-day interval between the first earthquakes and first phreatic explosion in March of 1980 (Endo and others, 1981; Malone and others, 1981). This similarity could indicate that a characteristic time interval exists between initiation of precursory activity and initial explosive activity at Mount St. Helens. If this is the case, then the time interval presumably is governed by the structure of the shallow conduit system and surrounding country rock, as well as the composition of the intruding magma.

Aside from the RSAM increase, there were no obvious precursors to the October 1 explosion. The explosion began aseismically, with no obvious changes in seismicity associated with the start of the explosion (Moran and others, this volume, chap. 6). Timing constraints for the explosion are excellent, because a CVO crew was flying around the vent when the explosion began (Schneider and others, this volume, chap. 17). The most obvious change in seismicity occurred at 1203, 1 minute after the explosion began, when earthquakes suddenly stopped (figs. 8, 9). This cessation was so dramatic that it caused one CVO crew working at seismic station STD (fig. 1) to look up at the crater when the sound of the earthquakes, heard through a scanner tuned to the frequency of a nearby seismic station, suddenly stopped. A relatively broadband

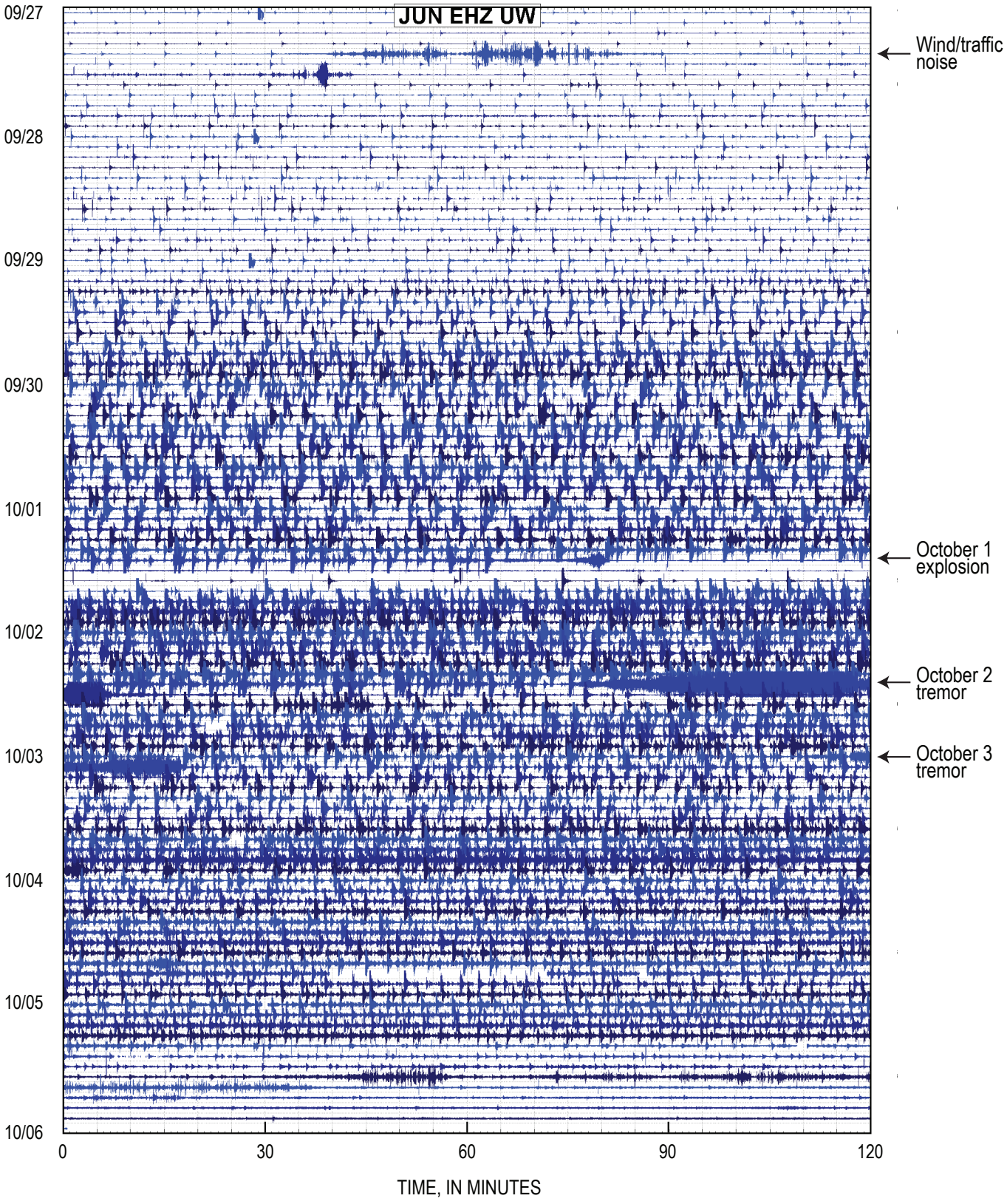


**Figure 8.** Seismic record from station JUN (6.5 km southeast of vent; fig. 1) from September 27 through October 5, 2004, showing seismicity trends during the vent-clearing phase.

(0.5–3 Hz) tremor signal accompanied the explosion after the last earthquake at 1203 (fig. 8), with tremor amplitudes roughly doubling between 1216 and 1221. At 1221 the tremor and the explosion stopped abruptly.

The October 1 explosion destroyed seismic station SEP, the closest station to the earthquakes (fig. 1). The loss of this station decreased the quality of PNSN catalog locations, with average hypocentral errors for well-constrained earthquakes (P waves on at least 7 stations, azimuthal gap <135°, nearest station within 3 km) increasing from 0.2 km in the 24 hours before October 1 to 0.34 km in the 24 hours after the explosion. This impact illustrates the importance of having seismic stations close to the source. Indeed, the loss of SEP was one of the primary motivations for the development of a seismic sensor package that could be remotely deployed at locations too hazardous for crews to work on the ground (McChesney and others, this volume, chap. 7).

## October 1–October 5, 2004

Seismicity levels dropped precipitously following the 1202–1221 explosive event, with the first small earthquake not occurring until roughly 3 hours later at 1515. This drop indicated that seismicity was occurring in response to elevated pressure in the conduit system, pressure that was temporarily reduced by the October 1 explosion. Hybrid earthquakes slowly increased in number and size and then rapidly increased between 1700 and 2000 on October 1, with RSAM levels eventually exceeding those of September 29–October 1. As with previous intensifications, RSAM levels flattened and then gradually declined on October 2 (fig. 9). At roughly 1217 PDT on October 2, earthquakes were replaced abruptly by relatively broadband seismic tremor with dominant frequencies in the 0.5–3-Hz range (fig. 10). Tremor rapidly intensified over a period of 20 minutes, to peak reduced-displacement values of 28–43 $cm^2$, and was energetic enough to be recorded on seismic stations more than 240 km away. The energetic tremor, in combination with the October 1 explosion and continuing energetic earthquake activity, caused CVO to issue a Volcano Alert, the highest alert level. No explosions or other obvious surficial events (such as increased steaming or small ash emissions) were observed in association with the tremor. Tremor amplitudes began decreasing shortly after the alert level change, and, by 1315, tremor had virtually disappeared. As with the October 1 explosion, earthquake rates and sizes decreased significantly after tremor ceased, although the drop was not as abrupt or as long-lived (figs. 8, 9, 10). Earthquake rates and sizes began increasing again around 1400, and by 1900 RSAM values had returned to levels just below those before the October 2 tremor episode (fig. 9). A smaller tremor episode (reduced displacement 10–20 $cm^2$, peak frequencies 0.5–2.5 Hz) occurred between 0250–0315 PDT on October

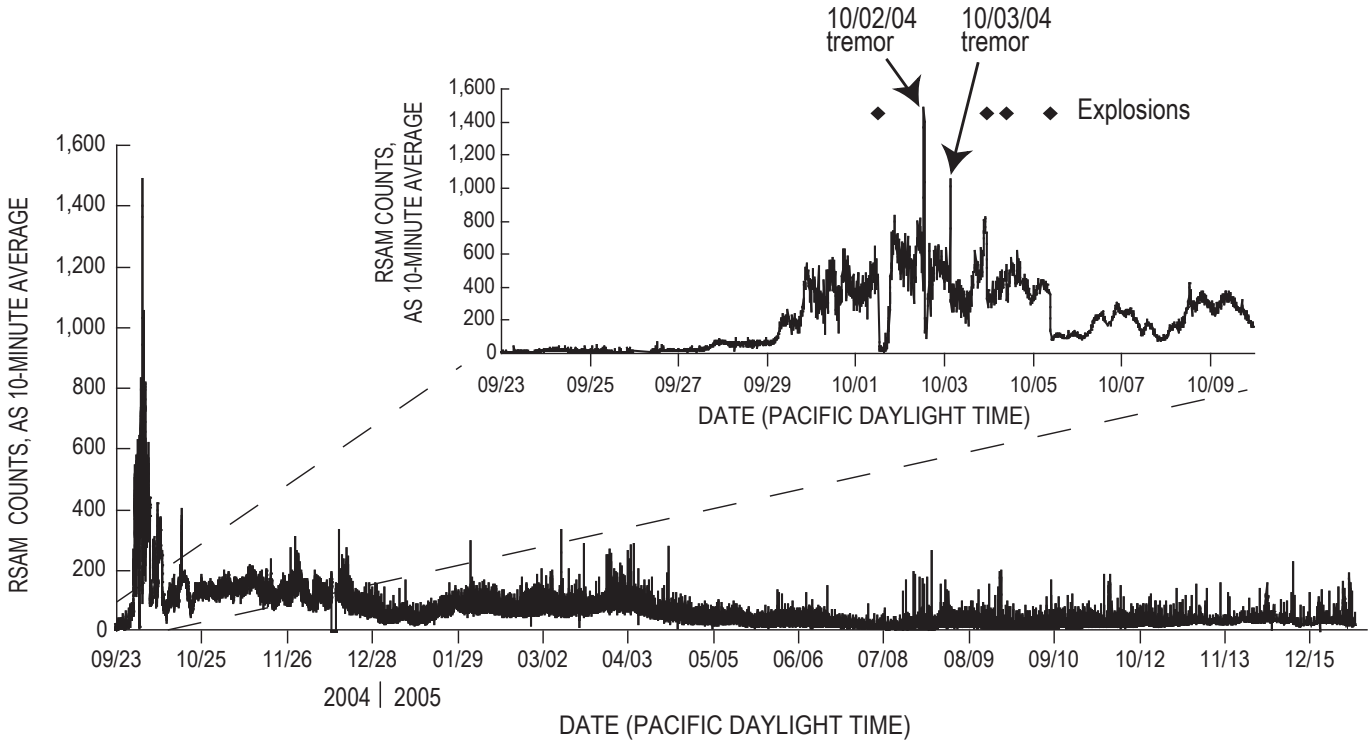


**Figure 9.** Plot of 10-minute real-time seismic amplitude measurement (RSAM) values from station SHW (3 km west of vent; fig. 1) between September 23, 2004, and December 31, 2005. Inset shows SHW RSAM between September 23 and October 10, timing of four phreatic explosions, and occurrence of two tremor episodes associated with a vent-clearing phase. Horizontal-axis tick marks in inset indicate start of a day, with gaps of 2 days between each tick mark.

3 (fig. 8), and, as with the October 2 episode, no eruptive plume was detected (M. Guffanti, written commun., 2004). In contrast to the October 2 episode, earthquakes continued to occur during the October 3 tremor episode. Although earthquake rates and RSAM levels dropped after the episode and remained low for the next 12 hours, the decrease was not as great as those that followed the October 1 explosion and the October 2 tremor.

Around 1500 PDT on October 3, earthquake rates again began increasing, with RSAM levels peaking at 1650 (fig. 9). After a brief drop, earthquake rates increased again, with seismicity dominated by many small-amplitude events. By 2100, earthquakes were occurring so close together in time that they became difficult to distinguish, forming a spasmodic tremor-like signal (fig. 8). Continuous, small-amplitude tremor was likely also occurring, although this signal can only be seen in the short gaps between individual earthquakes. Earthquake rates and the tremorlike signal decreased substantially around 2305, following a small steam-and-ash explosion at 2240 reported by U.S. Forest Service observers at the Coldwater Ridge Visitor Center, and RSAM dropped to levels similar to those from early in the day on October 3 (fig. 9). Following this small explosion, the number of larger ($M_d$ >2) earthquakes decreased, with many smaller hybrid earthquakes occurring in the gaps between larger events (fig. 8). Earthquake rates and RSAM levels gradually increased again until another steam-and-ash explosion at 0943 PDT on October 4, and, as before, earthquake rates and RSAM levels briefly dropped following the explosion (figs. 8, 9). Shortly afterward, RSAM levels increased again, peaked at 1700 on October 4, and then gradually declined to a relative low at 2330. As with roughly two-thirds of the previous RSAM increases, the peak and subsequent decline were not associated with explosions or other anomalous surface activity. RSAM levels increased once again beginning at 0000 PDT on October 5, reaching a peak at 0600 that was maintained until the final explosion of the vent-clearing stage began at 0903. Earthquake sizes and rates began declining ~15 minutes after the explosion began and continued to decline over the next hour as the explosion continued through 1015. After the explosion, RSAM levels were lower than at any time since September 29, with the exception of the lull following the October 1 explosion. Although RSAM levels increased and decreased several times over subsequent weeks, they never again reached levels achieved before the October 5 explosion (fig. 9).

Between September 29 and October 5, earthquakes were too large and occurring too close together in time for more than a fraction of all earthquakes to be detected and located by the PNSN. Using the average event rates given above, we estimate that ~30,000 earthquakes occurred over these seven days. The largest located event was a $M_d$ 3.9 on October 1, and 9 events had $M_d \geq 3.5$ between October 1 and October 4. To estimate the total amount of seismic energy expended during the vent-clearing phase, we calibrated RSAM values at station FMW (91 km north of Mount St. Helens) using 20 of the largest earthquakes and then integrated RSAM values from FMW between September 23 and October 5. The result was a cumulative magnitude equivalent to a $M_d$ 5.5 earthquake, an order of magnitude lower than the cumulative magnitude of $M_d$ 6.5 estimated for the March 28–May 18, 1980, precursory seismicity.

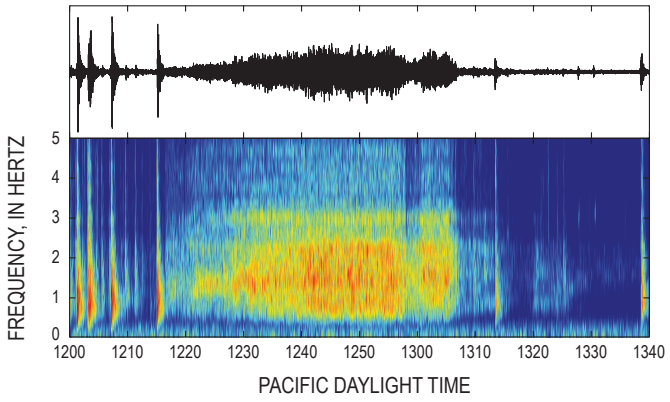


**Figure 10.** Tremor episode on October 2, 2004, as recorded on vertical component of broadband station JRO (8 km north of the vent; fig. 1). Time series (above) and spectrogram (below) for same time period. Note that discrete earthquakes stopped when tremor started at 1217 PDT and were significantly diminished after it ended at 1310.

## October 5, 2004–December 31, 2005: Seismicity Accompanying Dome Building

The steep decline in seismicity following the October 5 explosion caused CVO to lower its alert level to Volcano Advisory (Alert Level 2), where it remained through the end of 2005. Although RSAM levels increased again between October 6–7 and October 8–9, 2004, as a result of increasing event sizes (largest were $M_d$ 2.5–3.0), the increases were much more gradual and didn't reach September 29–October 5 levels (fig. 9). Because there had been a number of more rapid increases in seismicity between September 29 and October 5 that were not directly associated with eruptive activity, we did not change our alert status at the volcano during these more gradual intensifications. We noted during both those periods that earthquakes were dominated by a single event family, an attribute of Mount St. Helens seismicity that continues at the time of this writing (Moran and Malone, 2004; MacCarthy and Rowe, 2005; Thelen and others, this volume, chap. 4).

The October 8–9 earthquakes were a particularly spectacular example of an event family (fig. 11). Event magnitudes systematically increased over a ~12-hour period starting 0200 PDT, then stabilized at $M_d$ 2.5–3.0 for almost 24 hours before systematically declining over a ~12-hour period back to $M_d$ 1–1.5 (fig. 5). We generated hourly event stacks (fig.

11) to increase the signal-to-noise ratio of the P-wave arrivals and found that first motions were down at all stations, consistent with either very shallow reverse faulting or a deeper, nondouble-couple source (such as motion along a curved surface or an implosion). The appearance of event families, taken together with the overall decline in seismic levels, the change in event character to dominantly LF and hybrid events, the relatively low gas levels (Gerlach and others, this volume, chap. 26), and the observed deformation of the crater floor (Dzurisin and others, this volume, chap. 14), led CVO and the PNSN to believe that the most likely outcome was a new episode of lava dome building.

Seismicity declined significantly following the October 8–9 earthquake sequence. From October 10 to October 16, seismicity consisted of small ($M_d$ <1) events occurring at a rate of 1–2 per minute, as well as slightly larger events with longer between-event intervals. At 0200 on October 16 the number of discrete $M_d$ 1–1.5 events started decreasing, and between these events many tiny LF earthquakes appeared, spaced roughly 20 s apart (fig. 12). Event magnitudes of the tiny LF earthquakes steadily increased through October 17 before stabilizing at $M_d$ ~0.5. When first observing these smaller events we noted a strong similarity to short-lived episodes of tiny, closely spaced LF events that were observed at Mount St. Helens in three separate instances associated with the 1983–84 continuous dome-building eruption (R. Norris, oral commun., 2006). On the basis of this similarity, we inferred that these LF events likely represented the extrusion of a new dome.

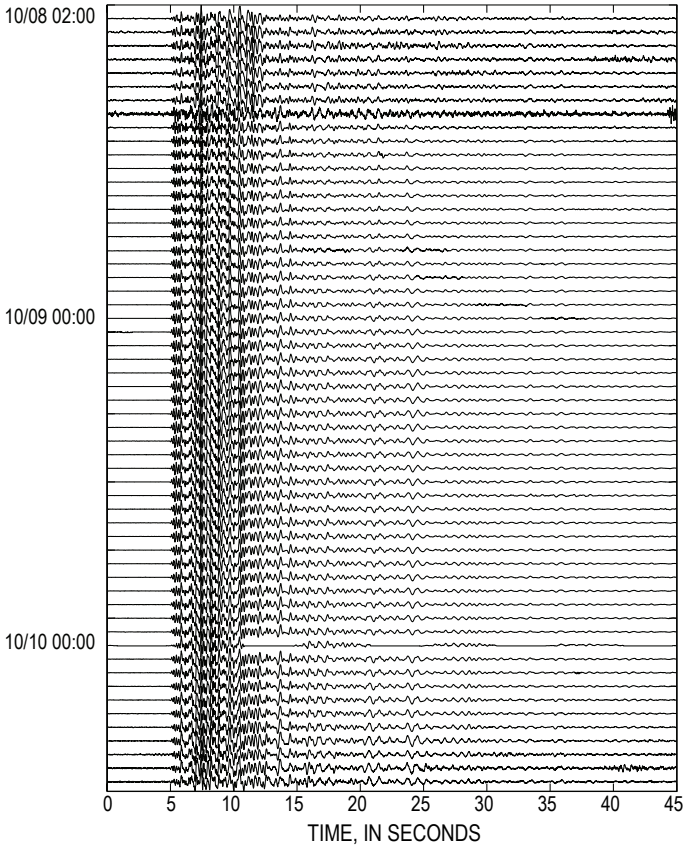


**Figure 11.** Plot of hourly stacks of events from earthquake family recorded on station HSR (2.5 km south of vent; fig. 1) between October 8 and October 10, 2004.

## "Drumbeat" Earthquakes

The appearance of regularly spaced, small earthquakes on October 16, 2004, marked the beginning of the next seismic phase of the eruption, a phase that continues at the time of this writing. Seismicity in this phase was dominated by these events, which occurred at such remarkably constant intervals that we dubbed them "drumbeat" earthquakes. The drumbeats consisted of repetitive LF and hybrid earthquakes and were one of the hallmarks of the eruption in 2004–5. Indeed, we know of no instances at other volcanoes when drumbeatlike events have been observed over such a long period of time. The drumbeats accompanied the regular rate of extrusion of several dacite spines (in this volume: Schilling and others, chap. 8; Vallance and others, chap. 9; Herriott and others, chap. 10; Poland and others, chap. 11; Major and others, chap. 12). Many of the drumbeats had waveforms similar to other drumbeats (Thelen and others, this volume, chap. 4), a similarity that can be used to relatively relocate events within individual earthquake families with high precision, as was done in the 1980s at Mount St. Helens by Frémont and Malone (1987). Thelen and others (this volume, chap. 4) present a thorough analysis of a number of well-recorded families. Identifying and relocating all earthquake families occurring within the million-plus earthquakes of late 2004 and 2005 is a large task that will likely take years to complete, well beyond the scope of this paper.

Several investigators have proposed models that link drumbeats and extrusion rate (Harrington and Brodsky, 2006; Iverson and others, 2006; Iverson, this volume, chap. 21; Mastin and others, this volume, chap. 22), with most invoking stick slip as the source mechanism. Horton and others (this volume, chap. 5) note that spectral peaks from drumbeats recorded on broadband stations deployed in 2004–5 are suggestive of resonance within a structure such as a crack or conduit, with resonance initiated by a stick-slip event (Neuberg and others, 2006) or by a pressure transient in a crack (Chouet, 1996). Research into the drumbeat source mechanism is ongoing, and it is not our intent to present a thorough discussion of possible drumbeat source mechanisms. Instead we focus on describing general trends in drumbeat event spacing, size, and frequency content and how changes in these characteristics correlated with dome extrusion.

### Event Spacing

Figure 13 shows that, to a first approximation, the time between drumbeats, or event spacing, changed little between October 16, 2004, and April 11, 2005, with daily averages ranging between 40 and 80 s. An important exception is that

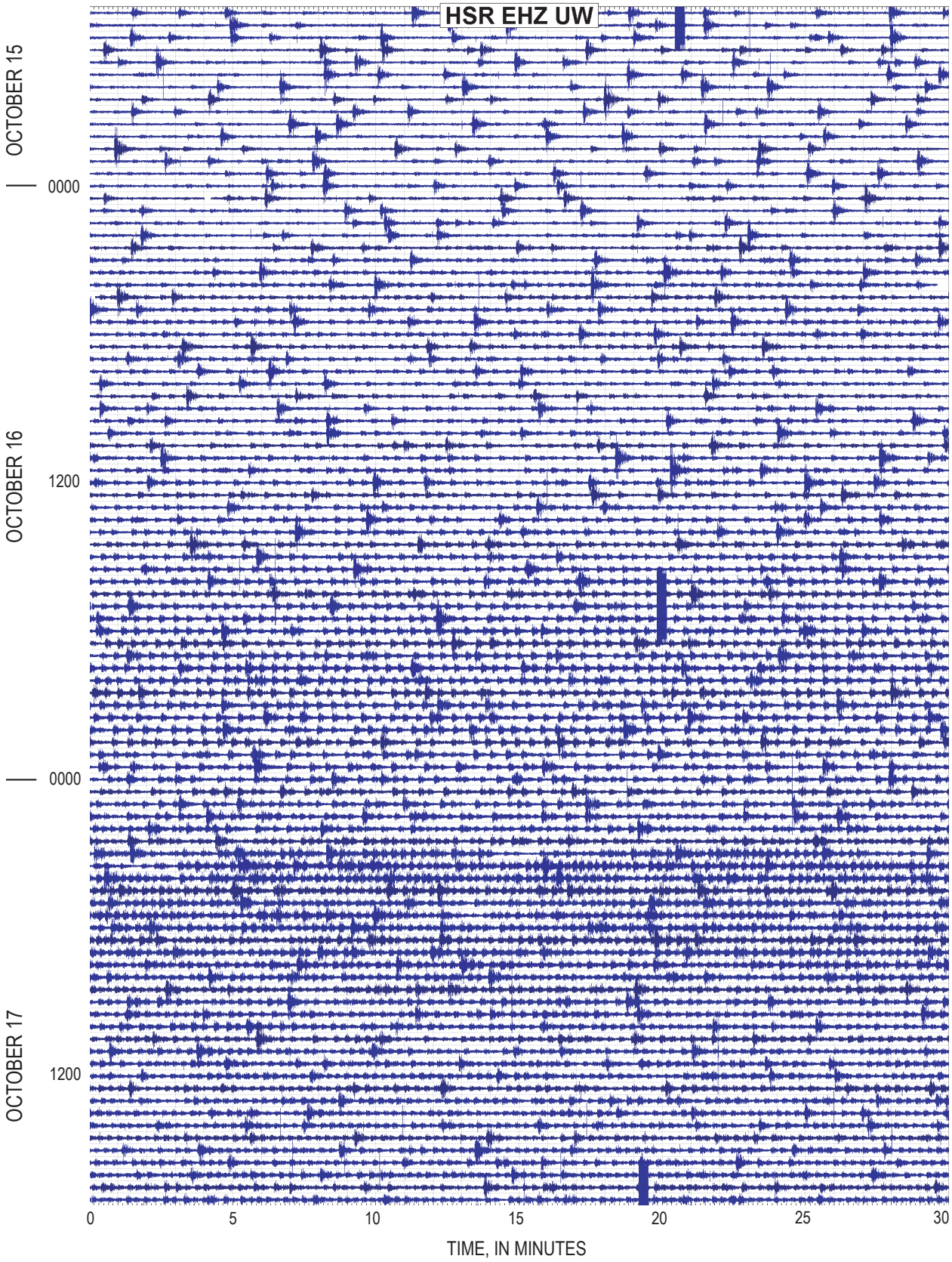


**Figure 12.** Seismic record from station HSR (2.5 km south of vent; fig. 1) from 1700 PDT on October 15 through 1800 PDT on October 17, 2004, showing onset of small, regularly spaced events ("drumbeats") occurring between larger events early on the morning of October 16. Drumbeat amplitudes increased gradually through the day.

between October 16 and November 12, 2004, events were occurring only ~20 s apart and were small enough that many went undetected by our detection algorithm (appendix 2). After November 12, event spacing increased to ~40 s, and visual inspections show that most events were detected. Between April 12 and July 8–10, 2005, the average event spacing gradually increased to more than 560 s, then briefly got shorter; on July 20 it became irregular, with spacing progressively increasing. In early August the events had become too small to be detected reliably by our algorithm on station HSR. Even on stations located within 1 km of the vent, earthquakes were occurring more as random earthquakes than drumbeats. By early October 2005, they had become so infrequent, emergent, and small that we began questioning whether the seismic events we were seeing were earthquakes or other surface sources, such as ice quakes and rockfalls. However, on October 9, 2005, earthquakes began to increase in size, and event spacing became remarkably regular again, with events occurring every ~70 s. Initially, event sizes were bimodal (fig. 13), with a population of larger-magnitude events (peak magnitude $M_d$ ~2.5) occurring alongside a population of more frequent smaller events. The larger-magnitude events gradually decreased in size until by mid-November 2005 there was just a single dominant event size. Event spacing began increasing in mid-December and, by the end of December 2005, had again become irregular.

One important qualification to the drumbeat story is that many small earthquakes recorded on stations located inside the crater in 2004–5 were not drumbeats. This was particularly the case from May through July of 2005, when the spacing between drumbeats increased significantly (fig. 13). As drumbeats decreased in size and number starting in mid-June, there was a factor of 15 difference between numbers of detected events at station MIDE (located ~200 m from the vent) and station HSR (2.5 km from the vent) between May 20 and July 18, 2005 (fig. 14). Some of the events detected at MIDE were rockfalls, but most were earthquakes that were too small to be recorded on stations >0.5 km from the vent. The

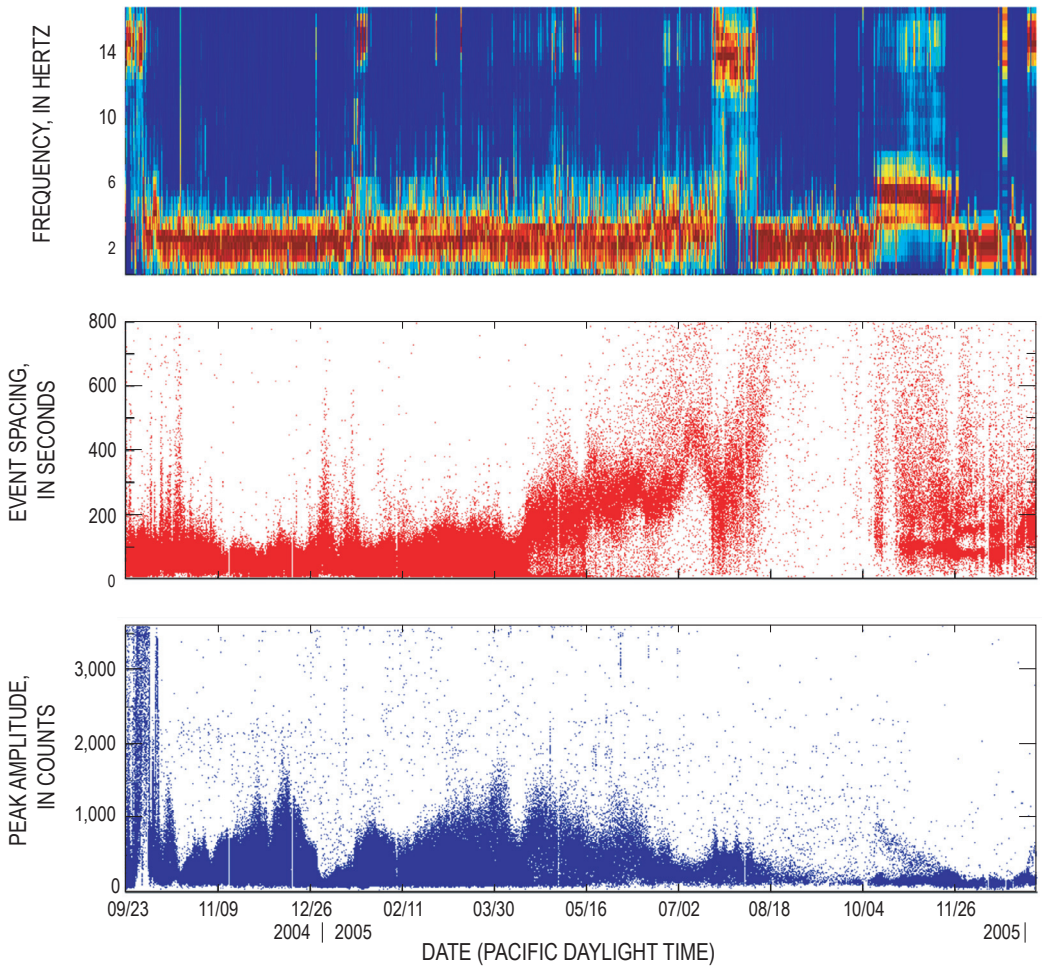


**Figure 13.** Plot showing ESAM (top), inter-event spacing (middle), and peak amplitudes (bottom) for detected events at station HSR (fig. 1) between September 23, 2004, and December 31, 2005 (see appendix 2 for event detection details). Roughly 370,000 events were detected during this time period, including occasional noise glitches and other false triggers.

events recorded on MIDE and other near-field stations lacked the regular spacing characteristic of drumbeats, and relative amplitudes and arrival-time patterns between MIDE and other near-field stations indicate that many were occurring within the extruded spines.

## Event Size Distribution

There was a complex relation between drumbeat event spacing and event size. In general, increases in event spacing corresponded to increases in event size and vice versa (fig. 15). For example, on December 16, 2004, average drumbeat magnitudes were $M_d$ ~1.5 and events were spaced ~90 s apart, whereas on December 23, 2004, average magnitudes had decreased to $M_d$ ~0.5 and events were spaced ~40 s apart (although occasional $M_d$ 1.0–1.5 events still occurred). If drumbeats are a result of stick-slip motion along a common fault plane and the steady extrusion rate corresponds to a constant slip rate (or stress accumulation rate) along the fault plane, then smaller drumbeats must be closer together if extrusion rate and seismic energy release are to remain constant. However, for seismic energy to have remained constant between December 16 and December 23, the event spacing would have had to decrease to ~3 s on December 23, a factor of 13 less than the observed ~40 s spacing. Thus there was a net reduction in seismic energy release between December 16 and December 23. Another drop in seismic energy release occurred in the evening of December 29, 2004, when drumbeat magnitudes dropped to $M_d$ 0.0–0.5 while event spacing remained roughly constant (fig. 13).

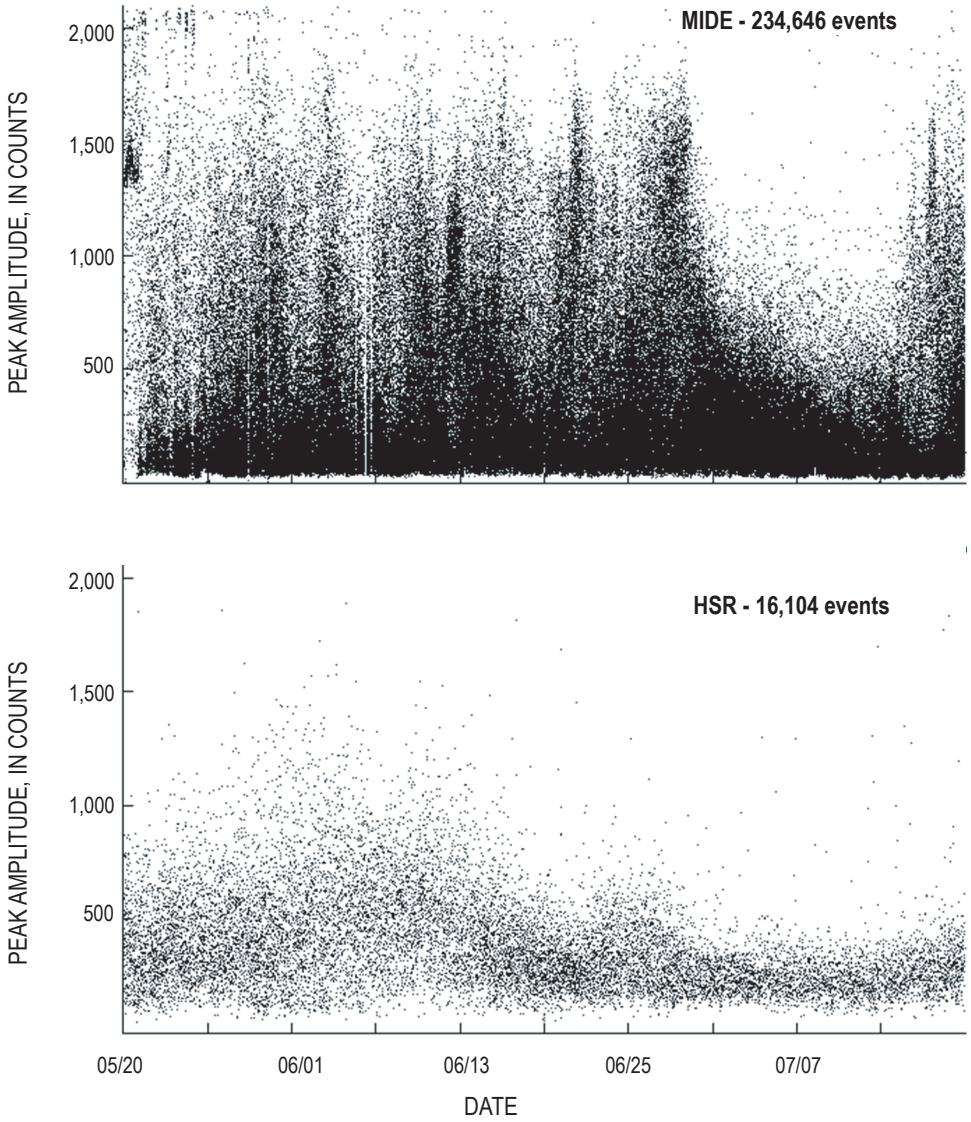


**Figure 14.** Detected events vs. time at stations MIDE (top) and HSR between May 20 and July 18, 2005. Note that the decline in events at HSR starting around June 13 is not seen at MIDE, evidence that many events detected on MIDE were occurring close to the station and were due to a process distinct from that responsible for the drumbeats.

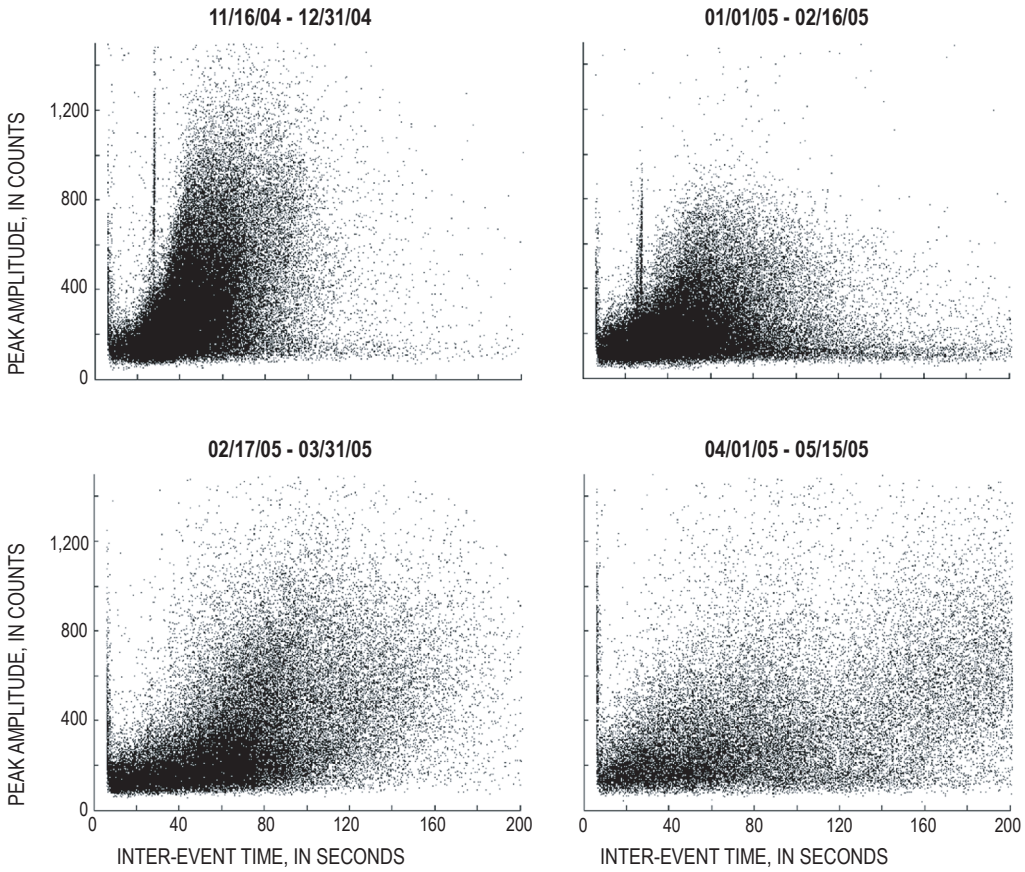


**Figure 15.** Plot of peak amplitudes vs. event spacing for detected events at HSR (fig. 1) for four time periods (all four plots have same vertical and horizontal scales). Although a general relation is seen between event size and inter-event time, particularly through mid-February (top two plots), the slope decreases over time, indicating that seismic energy release was declining as event spacing was increasing. Two linear features in the top two plots correspond to a sufficiently strong secondary phase arriving ~20 s after the P-wave at HSR to be occasionally detected as an event.

These and other decreases in seismic energy release could have been caused by decreases in extrusion rate, decreases in seismic coupling, or other changes in the mechanics of extrusion. Both December 2004 seismic energy drops (Dec. 23 and Dec. 29) occurred during the breakup of spine 3 and transition to spine 4 as the active locus of extrusion, a transition that began November 16 and continued through mid-January 2005 (Vallance and others, this volume, chap. 9). A mid-April 2005 drop in energy release, when event rates declined noticeably (fig. 13), coincided with the breakup of spine 4 and transition to spine 5, and another energy drop in mid-July coincided with the breakup of spine 5 and transition to spine 6 (Vallance and others, this volume, chap. 9). The correlation between transitions in extrusion style at the surface and changes in seismic energy release suggests that drumbeat seismicity was controlled to a certain extent by the mechanics of extrusion at the surface. Support for this interpretation comes from the observation that extrusion rates determined from digital elevation models (DEM) computed periodically throughout the eruption (Schilling and others, this volume, chap. 8) remained relatively constant despite fairly substantial changes in seismic energy release. In particular, the extrusion of spine 6 was associated with a significant drop in event rate and size from mid-August through early October of 2005, as described above. However, three DEMs spanning August–October 2005 show that the rate of extrusion remained roughly constant during the lull in seismicity. This lack of correspondence indicates that the rate and size of drumbeats may have been more a function of changes in extrusion mechanics than changes in magma flux through the conduit. Changes in extrusion mechanics that could have influenced earthquake occurrence include changes in the angle of extrusion (which would affect clamping forces), changes in the locus of extrusion, and (or) changes in the frictional properties along the conduit margin through rate hardening/softening or other processes.

A further complexity in the relation between event sizes and event spacing is that, although there clearly were extended periods of time when larger drumbeat events were followed by longer gaps, there also were many instances when larger events were followed by short gaps and smaller events followed by larger gaps. This complexity is not predicted by models that marry drumbeats with the regular extrusion rate (Iverson and others, 2006; Iverson, this volume, chap. 21; Mastin and others, this volume, chap. 22). If the drumbeats were a result of a stick-slip source, then this complexity indicates that drumbeats at times occurred at multiple locations within a complex network of shear zones, with individual faults having individual loading and unloading histories somewhat independent of those on other faults. It remains to be seen if individual drumbeat families (Thelen and others, this volume, chap. 4) show a more direct relation between event size and event spacing.

A final general characteristic of drumbeat magnitudes was their magnitude-frequency distribution over time. Most commonly, drumbeats occurred with a single dominant event size and, in general, did not follow a Gutenberg-Richter rela-

tion. This is consistent with the repetitive nature of the drumbeats and implies that source dimensions, as well as location, varied little between individual drumbeats. However, there were also time periods when event amplitudes appeared to follow a Gutenberg-Richter relation (fig. 13), in the sense that a greater number of small events occurred than large events. We note that there is no relation between event size and event spacing during many of these time periods, which also implies that multiple seismic sources were active at the same time.

## P-Wave Spectra

With a thousand or more events occurring per day, it was difficult to notice changes in event character over time, although obvious variations from the norm, such as the sporadic occurrence of VT events, were noted, usually within hours. One means we used for tracking changes in drumbeat character was to plot event spectra over time (see appendix 2 for details). Earthquake spectral amplitude (ESAM) plots in figures 5 and 13 show that seismicity transitioned from hybrid events following the October 5 explosion to LF events by October 9 and was dominated by LF events (peak frequencies in the 2–3-Hz range) through early January 2005. Between January 8 and 25, hybrid events occurred along with LF events (fig. 16), with peak hybrid P-wave frequencies of 8–16 Hz on station HSR. Hybrids also occurred with LF events between mid-April and late May 2005 and were the dominant event type between July 20 and August 11, 2005 (fig. 16). In both cases, peak P-wave frequencies were in the 12–16-Hz range on station HSR. Hybrids again occurred alongside LF events between October 9 and November 18, with peak P-wave frequencies in the 4–6-Hz range and a weaker band between 14 and 16 Hz (fig. 13). These frequency changes are most notable on stations HSR and SHW, two stations located 2.5–3 km from the vent. Changes in event appearance are also apparent on station YEL, ~1 km from the vent (the closest station to have operated throughout the entire eruption), but peak frequencies for the hybrid events are 4–5 Hz, suggesting that the path to YEL attenuates much of the high-frequency energy apparent on flank stations.

The four instances of concentrated hybrid occurrence all coincide with transitions in spine extrusion, as well as with several changes in event amplitude and (or) event spacing described above. The best example of this was July–August 2005, when seismicity switched from dominantly LF to dominantly hybrid events. A time-lapse sequence of photos (fig. 17) from a remote camera located on the northeast edge of the crater (Poland and others, this volume, chap. 11; Major and others, this volume, chap. 12) shows that the hybrid events began as the south end of spine 5 stopped moving on July 20, resulting in differential motion within the spine. As time progressed, the resultant shear zone moved northward, until finally spine 6 split away from spine 5 and began moving westwards around August 9–10. Other major spine transitions occurred December 2004–January 2005, mid-April 2005, and early October 2005 (Vallance and others, this volume, chap. 9). Hybrid seismic events occurred to varying degrees during each of these transitions, a correlation that suggests a direct relation between hybrids and motion of the spines after extrusion from the vent. One speculative model is that the hybrids are a result of differential shearing occurring along the base of the spine during spine transitions, whereas the LF events, which do not have as clear a relation to changes in spine motion after extrusion, occur at shallow depths along the conduit margin.

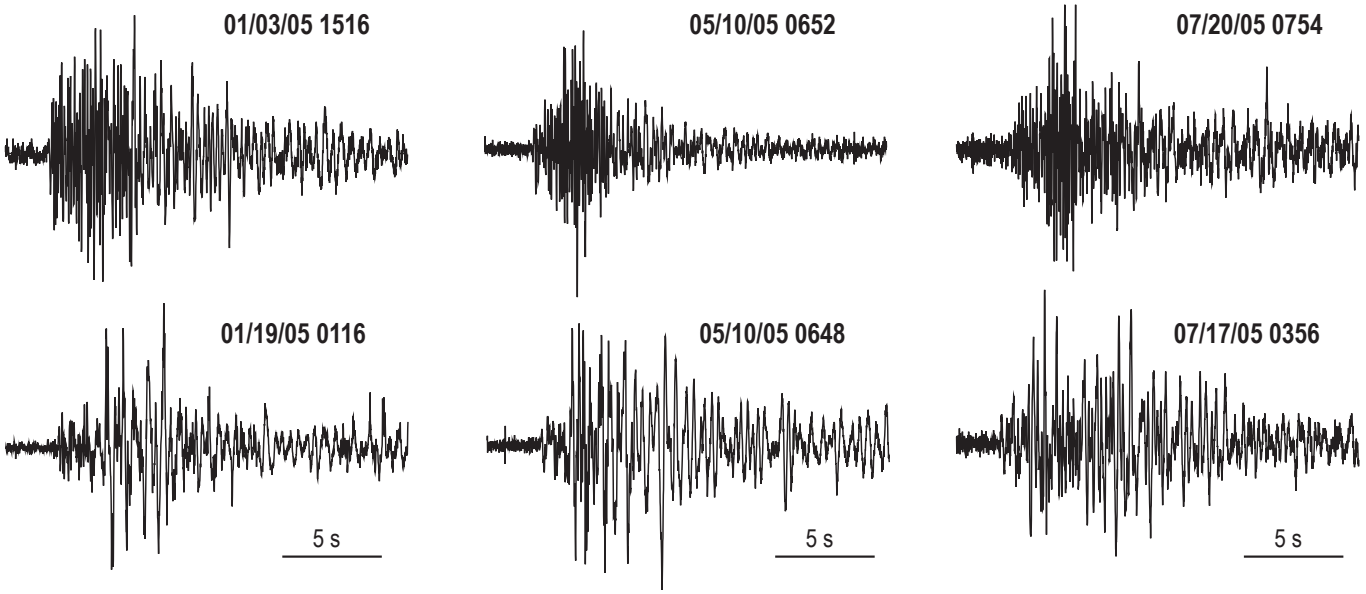


**Figure 16.** Examples of hybrid (top) and low-frequency drumbeats (bottom) as recorded at station HSR in January, May, and July 2005. Hybrid drumbeats were relatively rare and occurred in temporal clusters that are clearly visible on the ESAM plot in figure 13. Such clusters corresponded to transitional periods when one spine became inactive and a new spine began to grow.

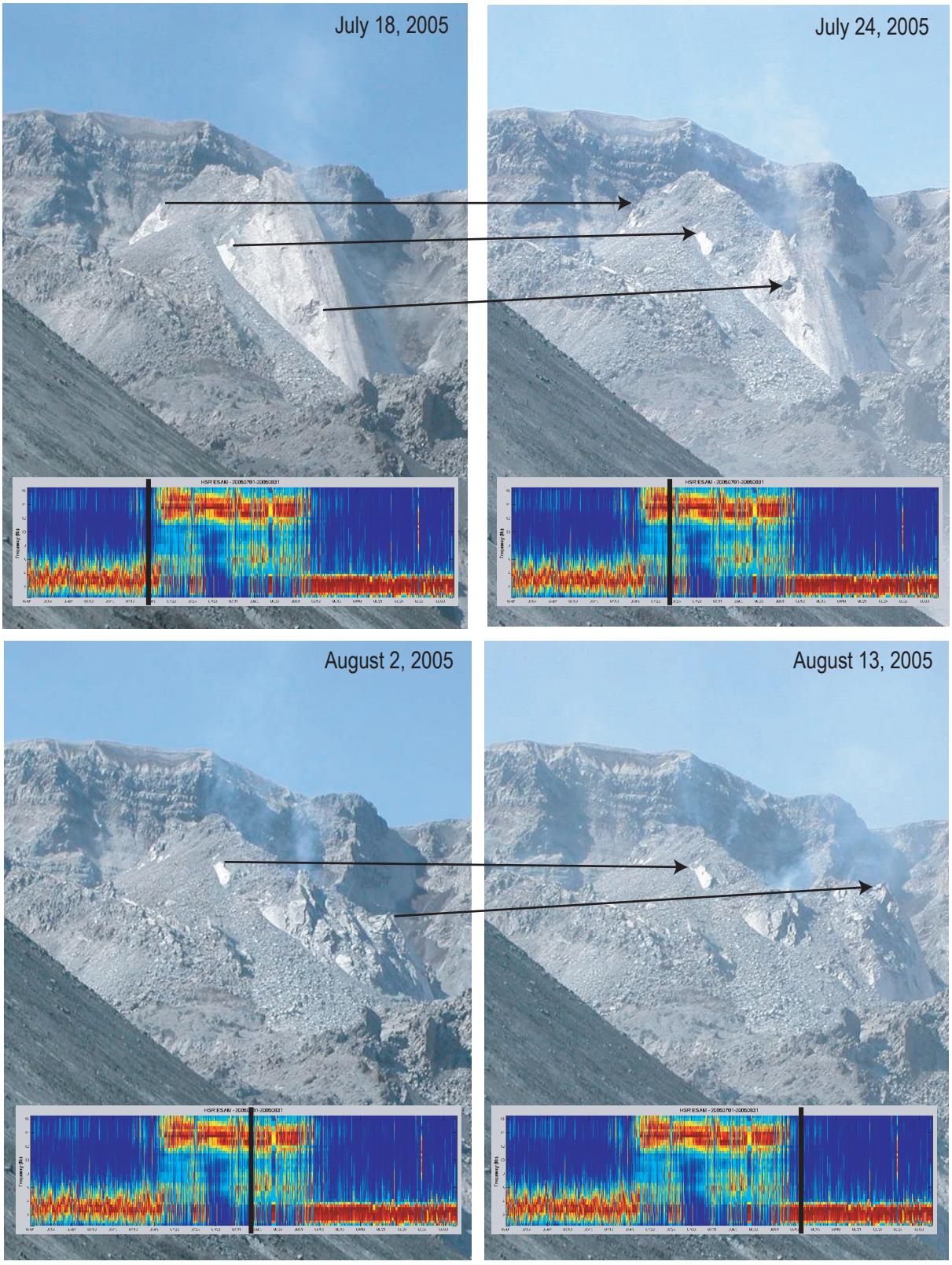


**Figure 17.** Four pictures taken from a camera station at SUG (fig. 1) showing transition from spine 5 to spine 6 that took place in late July–early August. Arrows indicate relative motion of common spots on spine 5. At bottom of each picture is an ESAM plot showing earthquake spectra between July 1 and August 31, 2005, with frequency ranging from 0 to 16 Hz (identical scale to figs. 5 and 13). Black vertical bar on each ESAM plot corresponds to date on which that picture was taken.

## "Big" Earthquakes

Another intriguing aspect of seismicity after October 16, 2004, was the occasional occurrence of larger, or "big" ($M_d$ >2.0, $M_{max}$ = 3.4), shallow earthquakes. The first of these was a $M_d$ 2.4 earthquake at 2048 PST on November 15, 2004, that was followed by 11 others over the next two weeks (fig. 18). These earthquakes were notable because they were much larger than the regular drumbeat events (fig. 19). They generated much interest among scientists and with the public, because they could be seen easily in the real-time digital helicorder plots displayed on the PNSN Web site (Qamar and others, this volume, chap. 3). Also, they often caused large rockfalls that, in turn, generated ash plumes, which frequently rose above the crater rim. The onset of the "big" events coincided with spine 3 encountering the south crater wall, as demonstrated by DEMs (Schilling and others, this volume, chap. 8). Spine 3 was likely in a state of uniaxial compression at this point, and the coincidence of its south-wall impingement and the occurrence of larger events suggests a causal relation.

The larger events cannot be distinguished from larger drumbeat events on the basis of PNSN catalog magnitudes alone, because drumbeats tend to have long codas that yield overly large $M_d$ values relative to magnitudes determined using amplitudes. We therefore arbitrarily define larger events as those post-October 2004 events with amplitudes large enough to clip on station HSR. Through the end of 2005 there were more than 290 larger earthquakes with a cumulative magnitude of $M_d$ 4.4. Most events occurred in one of four temporal clusters: November 15, 2004–January 14, 2005; January 25–March 9, 2005; March 22–April 22, 2005; and July 15–December 31, 2005 (fig. 18). The first and third clusters occurred in association with the breakup of spines 3 and 4, respectively, and the fourth occurred in association with the breakup of spines 5 and 6. In contrast, the second cluster occurred during steady extrusion of spine 4. The ends of the first and second clusters coincided with explosions on January 18, 2005, and March 8, 2005, respectively. The largest number of events in a single day was 11 on March 27, 2005, when several events occurred within an hour of their predecessors, and the largest daily moment release occurred April 4, 2005. Both peaks occurred during the transition in locus of active extrusion from spine 4 to spine 5.

Despite their size, the larger earthquakes are similar in several ways to the drumbeat events. Like the drumbeats, they are classified as either LF or hybrid events. Roughly 40 percent have impulsive arrivals on most stations, and, like the drumbeats, many of the events with impulsive arrivals have most or all down first motions (appendix 1). Many of the impulsive larger earthquakes have higher frequencies at the

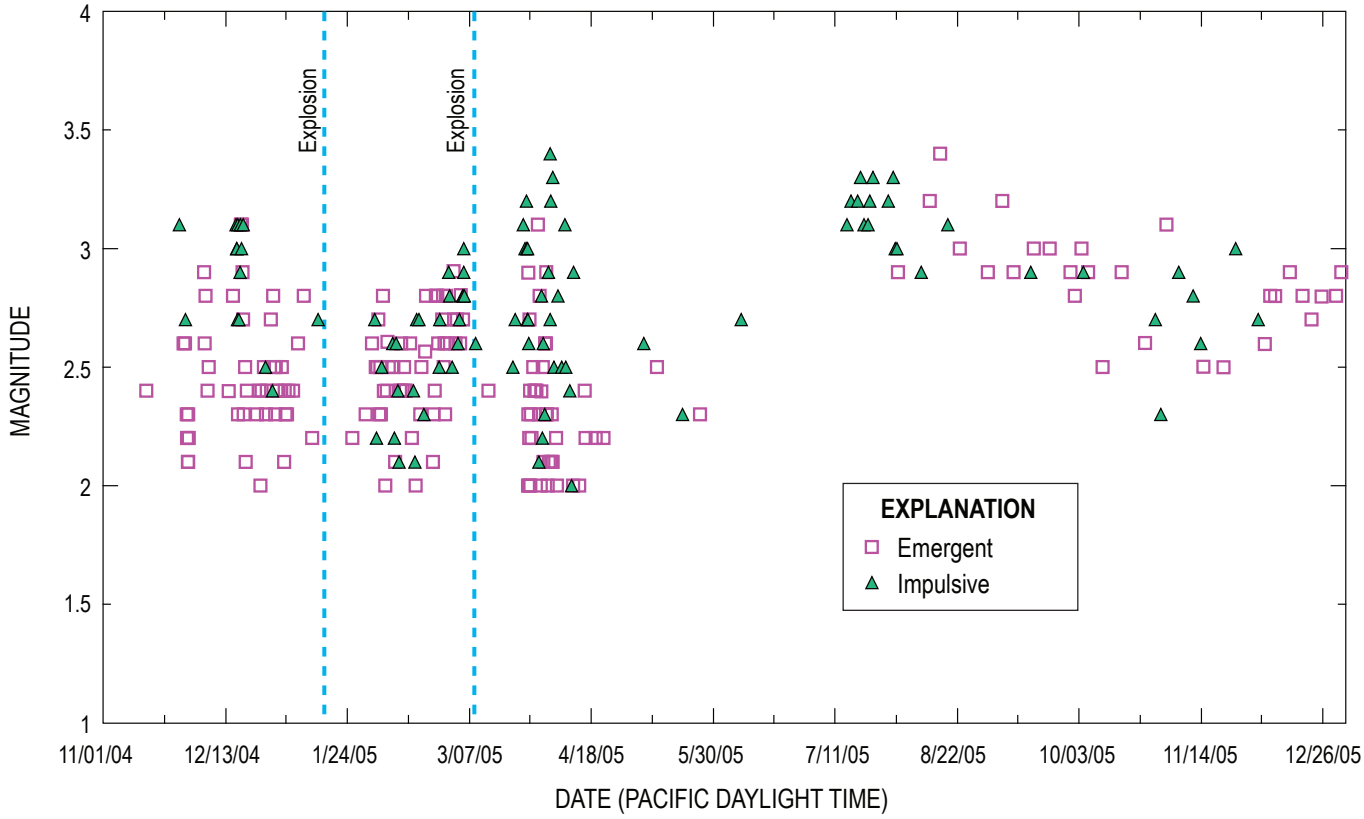


**Figure 18.** Plot showing occurrence of "big" earthquakes between November 1, 2004, and December 31, 2005. Green triangles correspond to impulsive events, hollow magenta squares to emergent events. Timing of two explosions on January 16 and March 8, 2005, are indicated by dashed blue lines.

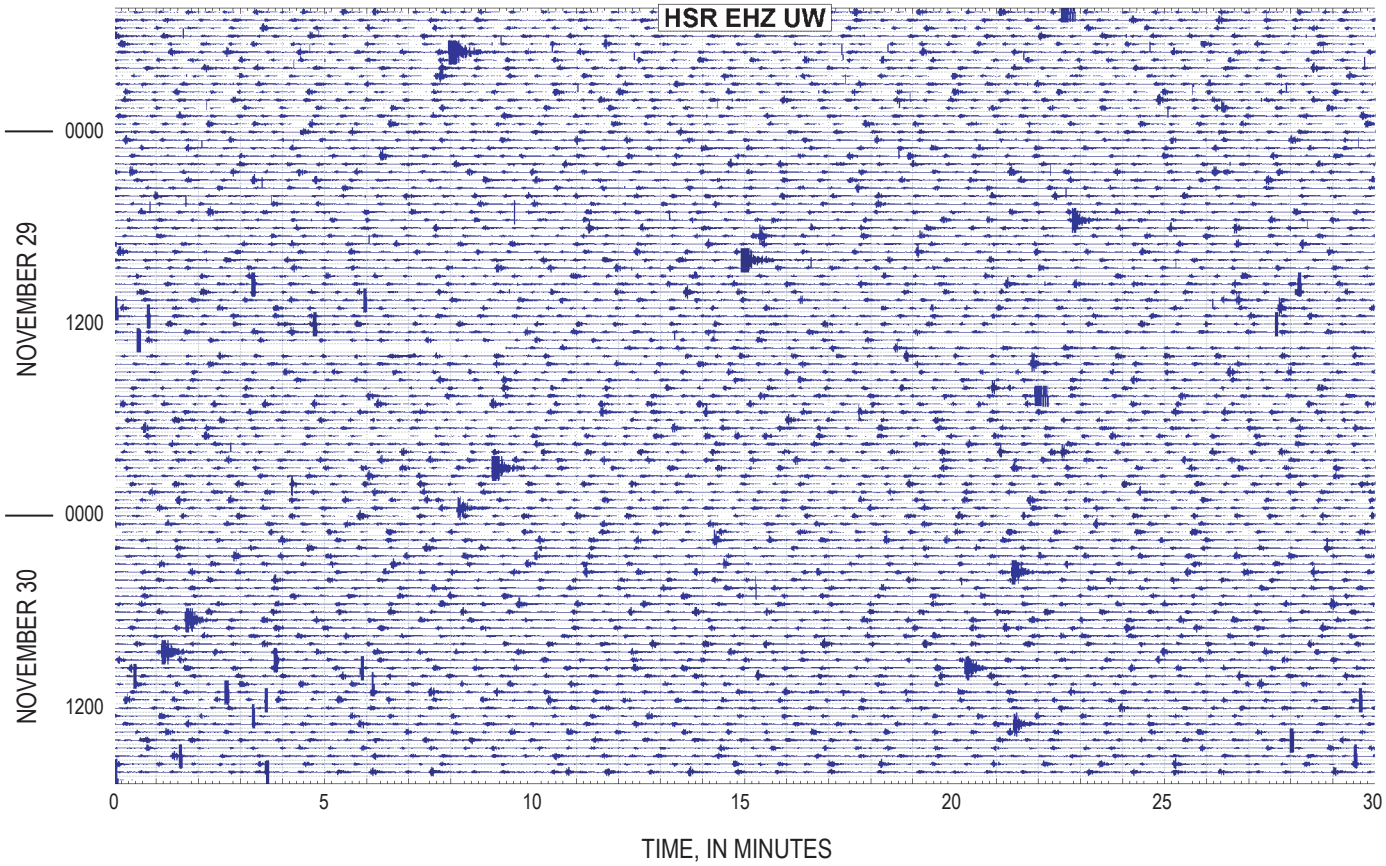


**Figure 19.** Seismic record from station HSR (see fig. 1) for 48 hours between 1700 PST on November 28 and 1700 PST on November 30, 2004, showing ten "big" earthquakes occurring along with regular drumbeats. Note that no change in drumbeat spacing or size occurs before or after the larger earthquakes, indicating that source processes are separate and distinct from one another.

start of the event and are classified as hybrid events, whereas the emergent events are dominantly LF events. Clipping of near-field sites makes event-family detection difficult, but on-scale recordings at broadband station JRO (~9 km from the vent; fig. 1) show that, although many of the larger events are dissimilar, there was at least one set of events occurring between December 2004 and April 2005 with similar waveforms (fig. 20). The similarity indicates not only that at least some of the larger earthquakes occurred in the same place with the same mechanism, but that the structure on which they occurred remained intact over a 4-month time span.

Spectra for drumbeats and the larger events are also similar. Figure 21 shows a set of waveforms and instrument-corrected spectra for a $M_d$ 1.0 drumbeat and a $M_d$ 3.0 "big" earthquake as recorded on stations plotted in order of distance from the earthquake. Spectra on all stations for both events have relatively flat curves for frequencies <1 Hz, a well-defined corner frequency at 1–2 Hz, and a $\omega^2$ decrease in frequency content at higher frequencies, all characteristics of tectonic earthquake spectra (Brune, 1970). Horton and others (this volume, chap. 5) found similar characteristics for events recorded on their broadband network in 2004–5. Of particular note is the nearly identical corner frequency ($F_c$ in fig. 21) of 1–2 Hz for all spectra, a frequency that is independent of distance and magnitude. One implication of this observation is that if the source is stick slip in nature, then the source duration is independent of source area. A source area independent of event size indicates that event magnitude is primarily a function of source displacement, rather than a combination of fault area and displacement as it is for tectonic earthquakes. This implies that the principal mechanical difference between drumbeats and "big" events is the amount of slip. If the earthquakes reflect stick-slip faulting within or at the periphery of the rising, rapidly solidifying magma plug (Iverson and others, 2006; Thelen and others, this volume, chap. 4; Iverson, this volume, chap. 21), then it is not surprising that the source area for these events is limited, because ruptures cannot propagate far outside of high-strain regions. The source duration of such a stick-slip event would then be a combination of the duration of motion of any part of the rupture surface and the area over which the rupture spreads, with the duration of this spreading being a function of the rupture velocity.

Locations for the impulsive larger events are more concentrated than drumbeat locations (fig. 22), although epicenters are still spread over an area 1 km by 1 km centered on the vent. Some of this scatter is likely due to changes in station

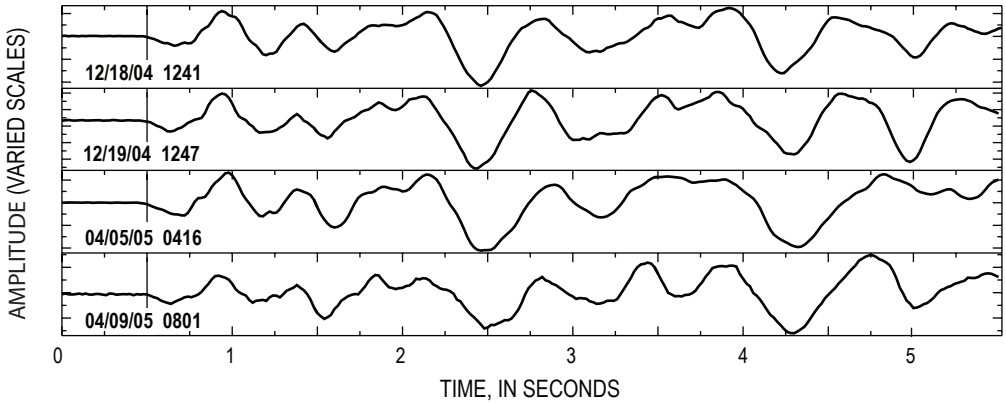


**Figure 20.** P-wave arrivals at broadband station JRO (fig. 1) for four "big" events occurring in December 2004 (upper two records) and April 2005 (lower two) with similar waveforms. Waveforms are scaled relative to the peak amplitude for each event. Although many "big" events do not have similar waveforms, the fact that some do indicates that these events on occasion occur at the same location with the same source mechanism. The 4-month time span between these four events also indicates that the structure on which these events occurred was not destroyed over that interval.

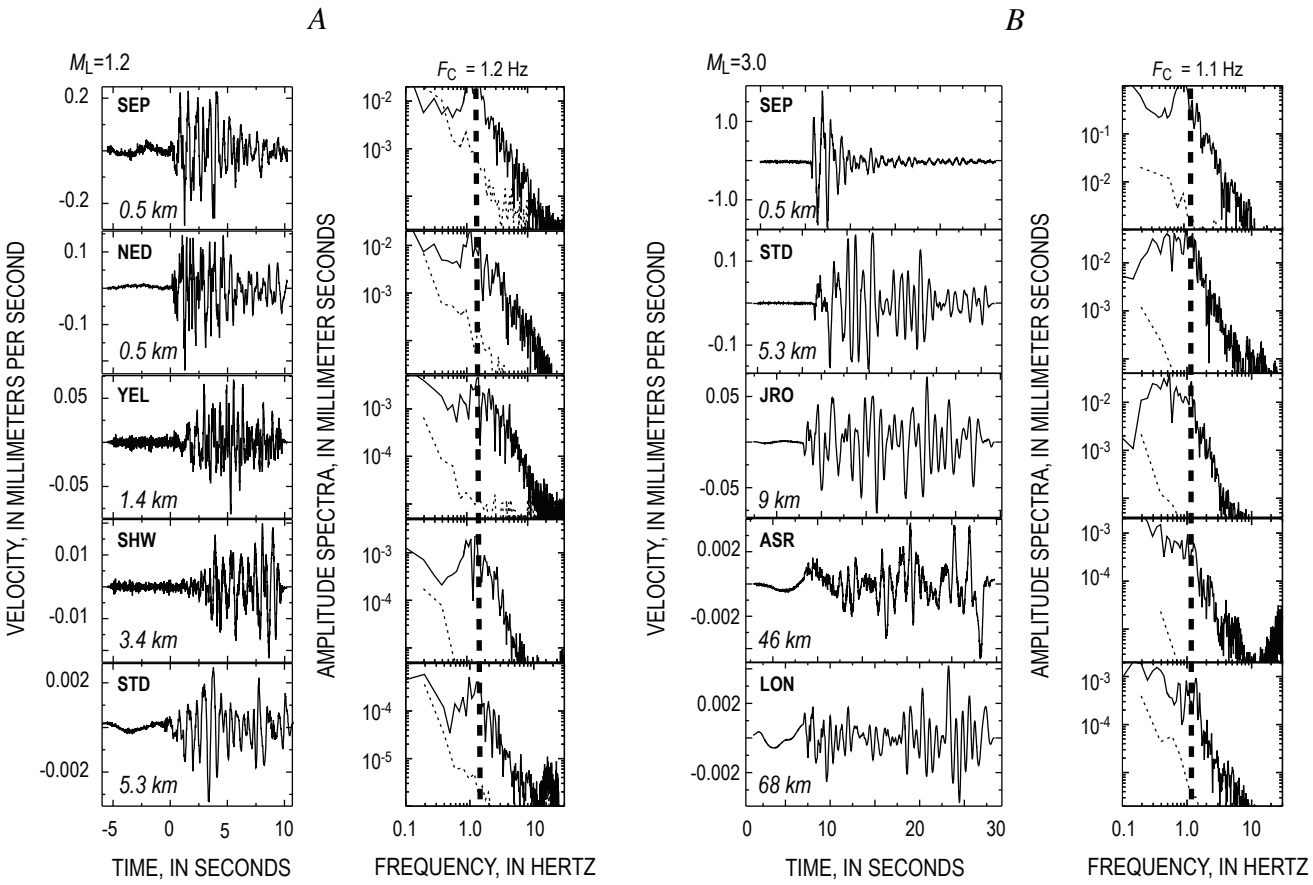


**Figure 21.** Instrument-corrected seismogram and frequency spectra for typical drumbeat (*A*) and "big" (*B*) seismic events. Stations are arranged in increasing distance from vent, with distance indicated for each station. All stations shown on location map (fig. 1) except ASR, located near Mount Adams, and LON, near Mount Rainier. Spectra are for 10.24-s windows starting with P-wave arrival. Thin dotted line below each spectral plot is noise estimate based on 10.24-s window taken before first arrival. Vertical thick dashed lines indicate corner frequencies ($F_c$) for each event. *A*, Drumbeat event, $M_L$ 1.2, on August 20, 2005, at 1345 PDT. *B*, "Big" event, $M_L$ 3.0, on March 26, 2005, at 1928 PST.

geometries and inaccuracies in the shallow velocity model (inaccuracies that, because of constantly changing velocity structure caused by the ongoing eruption, varied through time). Some scatter is also due to picking uncertainties, because arrival times, particularly on close-in stations, are difficult to pick to within ~0.1-s accuracy for all but the most impulsive events. However, some of the location scatter is real, the best evidence for which comes from differences in relative P-wave arrival times at stations placed close to the vent. As an example, figure 23 shows records on four crater stations from two events recorded ~9 hours apart on February 10 and 11, 2005. For the February 10 event, the P-wave arrived first at station BLIS (250 m east of the vent) and ~0.4 s later at AHAB (located 250 m southeast of the vent on top of spine 4); whereas for the February 11 event, the P wave arrived only 0.02 s later at AHAB. There was little change in relative P-wave arrivals at stations SEP and NED (~500 m north-northwest and ~500 m north-northeast of the vent, respectively). These patterns indicate that the February 11 event was located midway between AHAB and BLIS (350 m apart, including the altitude difference), whereas the February 10 event was located close to BLIS, a difference of as much as ~175 m (depending on P-wave velocities) between the two events. The 0.4-s difference in arrivals for the first event also implies remarkably low P-wave velocities (<1–2 km/s) at shallow depths, which is likely a result of AHAB and BLIS being placed on top of hot and highly fractured rock and crater-filling deposits (rockfall debris and ashfall deposits from the 1980 eruptions).

Hypotheses for the larger earthquake source include implosive-type mechanisms, fracturing of new rock (formation of new pathways to the surface), fracturing within spines before or after extrusion, and lurching of the active spine in a large-scale stick-slip event. Implosive mechanisms are consistent with all-down first-motion patterns observed for many of the impulsive events. However, none of these events occurred in association with explosions or significant degassing events. In addition, the extremely low levels of magmatic gases emanating from the vent (Gerlach and others, this volume, chap. 26) make it unlikely that sizable gas- or steam-filled cracks or pockets are able to accumulate below the surface and collapse to produce these events. We note, however, that Waite and others (2008) demonstrated that several events occurring in 2005 had a sig-

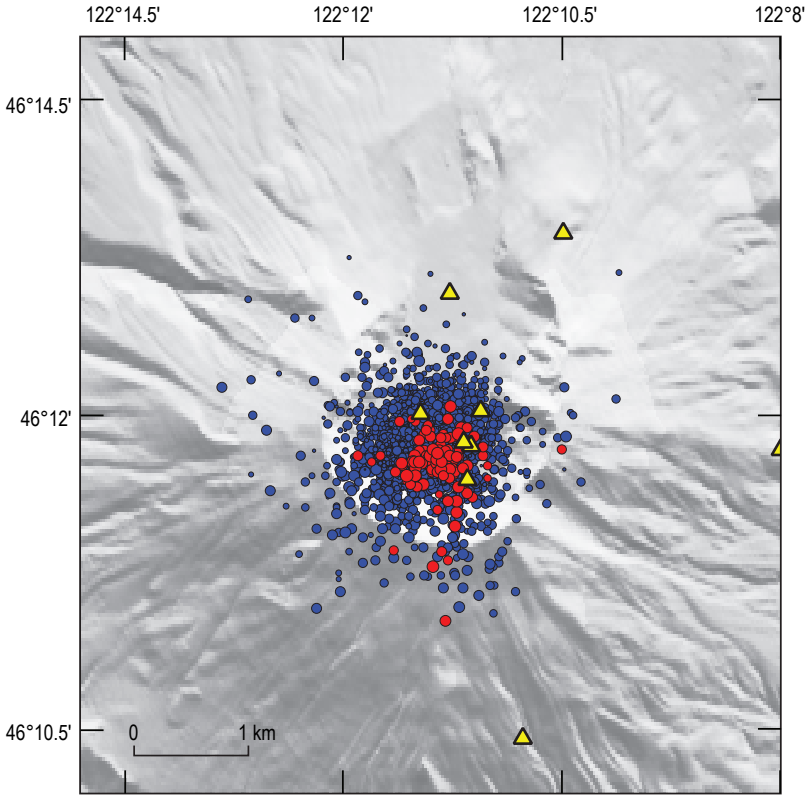


**Figure 22.** Map showing epicenters of drumbeat events (blue dots) and impulsive "big" events (red dots) occurring between November 1, 2004, and December 31, 2005. Dot sizes vary with magnitude. Drumbeat locations include events with P arrivals on at least seven stations, a nearest station within 2 km, and an azimuthal gap ≤135° (all impulsive "big" event locations meet these same criteria). Yellow triangles correspond to seismic station locations as of July 2005.

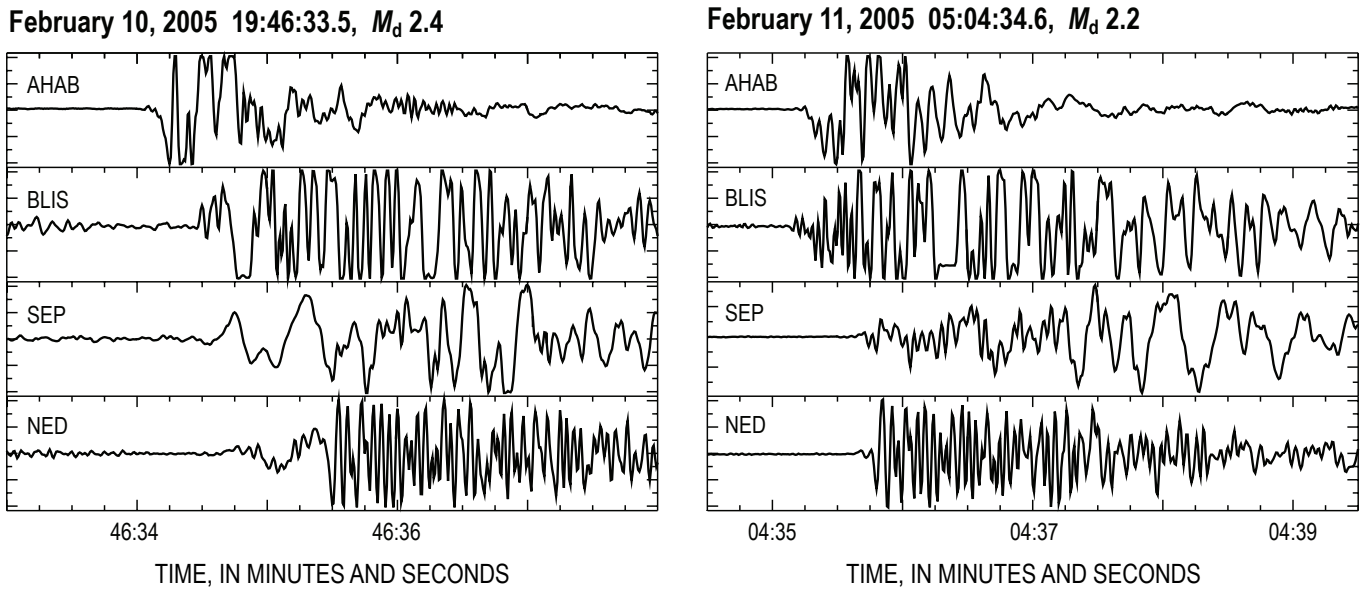


**Figure 23.** P-wave arrivals from two "big" earthquakes on four stations located within 0.5 km of vent (see fig. 1 for station locations). Note ~0.4-s difference in relative arrival times between stations AHAB and BLIS, indicating epicentral difference of more than one hundred meters for the two events.

nificant volumetric component, and they inferred that the source was a periodically collapsing, horizontal steam-filled crack.

Fracturing of new rock is also an unlikely process, as we would not expect to see repeating events or events with all-down first motions. Also, such a process would presumably not result in the emergent arrivals that we see at most stations in roughly half of the larger events. Fracturing within the spines is consistent with the observation that three of four large seismic-event clusters occur in association with the breakup of individual spines. However, events with all-down first motions are inconsistent with the observed failure mode in the spines, which occurred largely on shear, normal, and tensile fractures. Because the spines were, with one exception, higher than the seismometers, these failure modes would produce either a mixture of first motions or, in the case of normal faulting, dominantly up first motions. In addition, repetitive events spanning several months (and different spines) are incompatible with in-spine fracturing, because the fractures are destroyed in the spine breakup process.

Lurching of the active spine is our preferred hypothesis for the larger events. Lurches are consistent with shallow reverse faulting or upward thrusting of a piston that is indicated by the all-down first motions, as well as with long-lived event families. The fact that at least some events are located beneath the spine away from the vent indicates that they may have occurred along the interface between the base of the spine and the old crater floor. Because the 1980 crater floor is composed largely of ash and rockfall debris that fell from the crater walls in the years following the May 18, 1980, eruption, this interface likely is irregular and separates two poorly consolidated rock bodies. These lithologic and structural aspects could explain the emergent character of many larger seismic events and their low-frequency nature.

## Volcano-Tectonic (VT) Earthquakes

Following the initial VT-rich days of the vent-clearing phase, VT events were a minor component of seismicity at Mount St. Helens. On a daily basis we scanned through seismic records in search of VT events, because we felt that VT events, especially those deeper than 2–3 km, might be an indicator either of a surge of new magma entering the system or adjustment of the magmatic system to magma withdrawal—and thus a potential harbinger of the eruption's end. VT events occurred as isolated events throughout the eruption and had small magnitudes ($M_d$ <1), shallow (<2 km) depths, and epicenters similar to those for the drumbeats and larger events. The most notable occurrence of VT events was a swarm of more than 70 small ($M_d$ <0.3) shallow earthquakes occurring between December 27, 2005, and January 4, 2006. The VT events in this swarm occurred independently of the low-frequency drumbeats, in some cases occurring just tens of seconds before or after a drumbeat (fig. 24). This swarm appears quite clearly in figure 13, as only the VT events were large enough to pass our amplitude threshold for the ESAM plot during this time period. Poor weather obscured the volcano from view during this interval, but tiltmeters located on the 1980–86 lava dome showed slight inflation while VT events were occurring, in contrast to deflation before and after (D. Sherrod and M. Lisowski, oral commun., 2006). Other periods of inflation, however, do not coincide with VT events, so we are uncertain whether this relation is coincidental. Given the lack of correspondence of VTs to any obvious changes in eruption dynamics or mechanics of extrusion, our best guess is that the VT events represent fracturing of more competent rock in the crater floor, such as basaltic andesite

lava flows from the Castle Creek period (2,200–1,895 yr B.P.) that underlie much of the 1980 crater (Clynne and others, this volume, chap. 28).

## Summary—Patterns and Trends in Mount St. Helens seismicity, 2004–2005

In several intriguing ways the precursory seismic sequence of September 23 to early October 2004 was similar to those before the May 18, 1980, eruption and the 20 eruptions that followed during 1980–86. The 8-day-long interval between the first earthquakes and the first phreatic explosion on October 1, 2004, is close to the 7-day interval seen in March of 1980 (Endo and others, 1981; Malone and others, 1981), suggesting a characteristic time interval for magma to reach the surface once it begins to move. In addition, the transition from VT events to hybrid and LF events starting September 25, 2004, was broadly similar to transitions in event type seen before many of the dome-building eruptions in the 1980s (Malone, 1983). The occurrence of the event families, starting with the first significant family on September 26, 2004, is also similar to occurrence of event families before and during 1983–86 dome-building eruptions (Frémont and Malone, 1987), as well as to those in association with many other dome-building eruptions (for example, Okada and others, 1981; Power, 1988; Power and others, 1994; Villagómez, 2000; Rowe and others, 2004). In retrospect, the combination of event-type transition and occurrence of event families on September 25, 2004, could have given us an early indication of the expected nature of eruptive activity at Mount St. Helens, although that knowledge would likely not have changed how CVO and the PNSN reacted to the developing seismic crisis.

A summary observation from the September 29–October 5 period is that, of the hours-long increases in seismic intensity, only 4 of 12 occurred before explosions (fig. 9). Furthermore, seismic energy levels had stabilized at least an hour before two of the four explosions (October 1 and October 5). Thus we find no statistical basis for using short-term increases in RSAM or other measures of seismic energy to make short-term forecasts of explosive activity.

The drumbeats and “big” earthquakes associated with the dome-building eruption represent a relatively new type of seismicity at Mount St. Helens that, with a few exceptions, was not a dominant characteristic of 1980–86 seismicity. Efforts

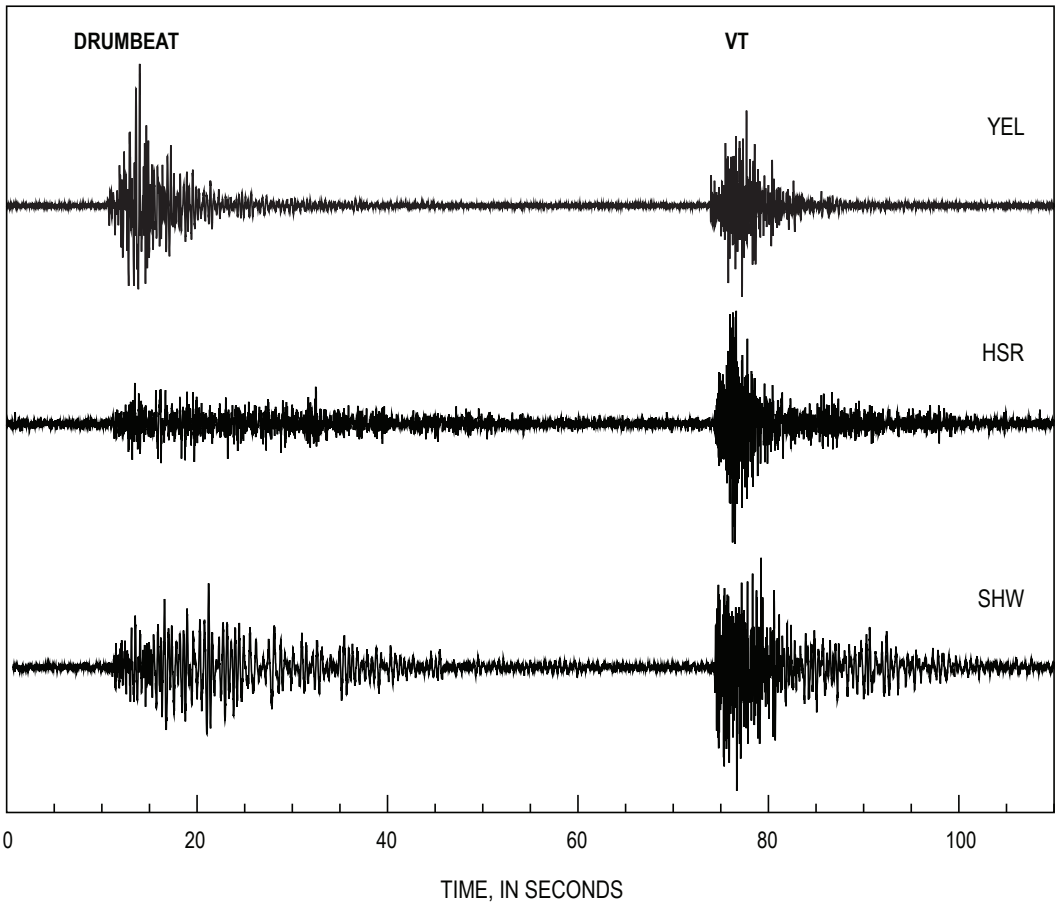


**Figure 24.** Seismograms from three stations for a drumbeat and a VT event occurring within 50 s of each other on December 29, 2005, at 1643 and 1644 PST, respectively. See figure 1 for station locations.

to characterize the nature of the drumbeat source are ongoing and likely will be the subject of research papers for years to come. Relatively new results with fascinating implications have already emerged from several field experiments run during 2004 and 2005, including the finding of infrasonic pulses associated with some drumbeats (Matoza and others, 2007) and the discovery of very long period (VLP) earthquakes in association with some of the larger drumbeats (Waite and others, 2008). These results provide evidence that processes operating at both deep (~500 m) and shallow (surface) levels are involved in the generation of drumbeats. The complexities in the relation between event spacing, event size, event spectra, and extrusion rate discussed in this paper, as well as in Thelen and others (this volume, chap. 4), further illustrate that the drumbeat source process is complex.

Finally, an important lesson that was reemphasized by the rapid escalation of seismicity during the first week of the eruption is that conditions can quickly become too dangerous to deploy additional seismometers after a volcano awakens. We were fortunate that the Mount St. Helens network installed in 1980–1983, particularly crater stations SEP (formerly REM) and YEL, was still in place and functional in 2004, because many of the events from the first two days were poorly recorded on stations outside of the crater. As the seismic crisis progressed, however, the limited dynamic range of the short-period analog stations was frequently exceeded at seismometers in the crater and on the flanks, resulting in lost information about seismic energy, spectral content, and event similarity. In addition, the absence of broadband three-component instruments in the crater meant that information was lost about the presence or absence of very low frequency signals and about source mechanisms for all types of events. As discussed by McChesney and others (this volume, chap. 7), seismicity intensified so rapidly during the first several days that we were unable to safely install such instruments in the crater. An important goal for seismic monitoring networks at any potentially active volcano should be to have seismometers, including broadband seismometers, installed at locations close to the presumed vent well before unrest begins.

## Acknowledgments

The number of people involved in the seismic response to the renewed eruption in 2004–5 was huge, and it is impossible to give proper credit to all who helped us. Peggy Johnson, Josh Jones, Ruth Ludwin, Wendy McCausland, Karen Meagher, Guy Medema, Bob Norris, Bill Steele, George Thomas, and Tom Yelin all played critical roles in the PNSN/CVO seismic monitoring team, particularly with the immense tasks of data processing, production of Web graphics, around-the-clock monitoring of seismicity in the first several months of the eruption, and troubleshooting hardware problems brought on by the immense amount of seismic data and Web traffic. Marv Couchman, Rick LaHusen, Andy Lockhart, Jeff Marso, Pat McChesney, and Tim Plucinski all played critical roles in developing and installing new seismic and telemetry systems on and around the volcano, and we are extremely grateful to each of them for the many hours they devoted to improving real-time seismic monitoring at the volcano. Wendy McCausland calculated reduced displacement estimates for the October 2 and October 3 tremor episodes, and Bob Norris assisted with overnight shifts at CVO for more than a month, provided logistical support in the field, and was the first to recognize the similarity between 2004 drumbeats and “peppercorn” events seen in the 1980s.

We are grateful to Peter Cervelli for providing invaluable assistance in the drafting of all figures showing multiday seismic records and to Dave Ramsey for providing us with the station map showing crater station locations superimposed on the April 19, 2005, DEM in figure 1. We thank Jeff Johnson for his assistance with event-family identification during the first several weeks of the eruption and Helena Buurman for her assistance in processing and error-checking the results from our earthquake detection algorithm. We also thank Phil Dawson, John Power, Stephanie Prejean, and Randy White for their contributions to analysis and discussions of the significance of seismicity during the first critical weeks of renewed activity, for forming invaluable bridges to other researchers in the volcano seismology community when we were too busy to do so, and for providing greatly appreciated moral support during the first incredibly hectic weeks of the eruption. Finally, we are grateful to Charlotte Rowe and Randy White for thorough reviews that significantly improved this paper.

## References Cited

Barker, S.E., and Malone, S.D., 1991, Magmatic system geometry at Mount St. Helens modeled from the stress field associated with posteruptive earthquakes: Journal of Geophysical Research, v. 96, no. B7, p. 11883–11894, doi:10.1029/91JB00430.

Bender, B., 1983, Maximum likelihood estimation of *b* values for magnitude grouped data: Bulletin of the Seismological Society of America, v. 73, p. 831–851.

Brune, J.N., 1970, Tectonic stress and the spectra of seismic shear waves from earthquakes: Journal of Geophysical Research, v. 75, no. 23, p. 4997–5009.

Chouet, B.A., 1996, Long-period volcano seismicity; its source and use in eruption forecasting: Nature, v. 380, p. 309–316.

Clynne, M.A., Calvert, A.T., Wolfe, E.W., Evarts, R.C., Fleck, R.J., and Lanphere, M.A., 2008, The Pleistocene eruptive history of Mount St. Helens, Washington, from 300,000 to 12,800 years before present, chap. 28 *of* Sherrod, D.R., Scott, W.E., and Stauffer, P.H., eds., A volcano rekindled;

the renewed eruption of Mount St. Helens, 2004–2006: U.S. Geological Survey Professional Paper 1750 (this volume).

Dzurisin, D., Vallance, J.W., Gerlach, T.M., Moran, S.C., and Malone, S.D., 2005, Mount St. Helens reawakens: Eos (American Geophysical Union Transactions), v. 86, no. 3, p. 25, 29.

Dzurisin, D., Lisowski, M., Poland, M.P., Sherrod, D.R., and LaHusen, R.G., 2008, Constraints and conundrums resulting from ground-deformation measurements made during the 2004–2005 dome-building eruption of Mount St. Helens, Washington, chap. 14 *of* Sherrod, D.R., Scott, W.E., and Stauffer, P.H., eds., A volcano rekindled; the renewed eruption of Mount St. Helens, 2004–2006: U.S. Geological Survey Professional Paper 1750 (this volume).

Endo, E.T., and Murray, T., 1991, Real-time seismic amplitude measurement (RSAM): a volcano monitoring and prediction tool: Bulletin of Volcanology, v. 53, no. 7, p. 533–545.

Endo, E.T., Dzurisin, D., and Swanson, D.A., 1990, Geophysical and observational constraints for ascent rates of dacitic magma at Mount St. Helens, *in* Ryan, M.P., ed., Magma transport and storage: New York, John Wiley, p. 317–334.

Endo, E.T., Malone, S.D., Noson, L.L., and Weaver, C.S., 1981, Locations, magnitudes, and statistics of the March 20–May 18 earthquake sequence, *in* Lipman, P.W., and Mullineaux, D.R., eds., The 1980 eruptions of Mount St. Helens, Washington: U.S. Geological Survey Professional Paper 1250, p. 93–107.

Fehler, M., 1985, Locations and spectral properties of earthquakes accompanying an eruption of Mount St. Helens: Journal of Geophysical Research, v. 90, p. 12729–12740.

Fehler, M., and Chouet, B.A., 1982, Operation of a digital seismic network on Mount St. Helens volcano and observations of long-period seismic events that originate under the volcano: Geophysical Research Letters, v. 9, no. 9, p. 1017–1020.

Frémont, M.J., and Malone, S.D., 1987, High precision relative locations of earthquakes at Mount St. Helens, Washington: Journal of Geophysical Research, v. 92, no. B10, p. 10223–10236.

Gerlach, T.M., McGee, K.A., and Doukas, M.P., 2008, Emission rates of $CO_2$, $SO_2$, and $H_2S$, scrubbing, and preeruption excess volatiles at Mount St. Helens, 2004–2005, chap. 26 *of* Sherrod, D.R., Scott, W.E., and Stauffer, P.H., eds., A volcano rekindled; the renewed eruption of Mount St. Helens, 2004–2006: U.S. Geological Survey Professional Paper 1750 (this volume).

Giampiccolo, E., Musumeci, C., Malone, S.D., Gresta, S., and Privitera, E., 1999, Seismicity and stress-tensor inversion in the central Washington Cascades mountains: Journal of Geophysical Research, v. 89, p. 811–821.

Harrington, R.M., and Brodsky, E.E., 2006, The Mount St. Helens hybrid earthquakes; stick-slip or resonating pipes [abs]: Eos (American Geophysical Union Transactions), v. 87, Fall Meeting Supplement, V52A-02.

Herriott, T.M., Sherrod, D.R., Pallister, J.S., and Vallance, J.W., 2008, Photogeologic maps of the 2004–2005 Mount St. Helens eruption, chap. 10 *of* Sherrod, D.R., Scott, W.E., and Stauffer, P.H., eds., A volcano rekindled; the renewed eruption of Mount St. Helens, 2004–2006: U.S. Geological Survey Professional Paper 1750 (this volume).

Horton, S.P., Norris, R.D., and Moran, S.C., 2008, Broadband characteristics of earthquakes recorded during a dome-building eruption at Mount St. Helens, Washington, between October 2004 and May 2005, chap. 5 *of* Sherrod, D.R., Scott, W.E., and Stauffer, P.H., eds., A volcano rekindled; the renewed eruption of Mount St. Helens, 2004–2006: U.S. Geological Survey Professional Paper 1750 (this volume).

Iverson, R.M., 2008, Dynamics of seismogenic volcanic extrusion resisted by a solid surface plug, Mount St. Helens, 2004–2005, chap. 21 *of* Sherrod, D.R., Scott, W.E., and Stauffer, P.H., eds., A volcano rekindled; the renewed eruption of Mount St. Helens, 2004–2006: U.S. Geological Survey Professional Paper 1750 (this volume).

Iverson, R.M., Dzurisin, D., Gardner, C.A., Gerlach, T.M., LaHusen, R.G., Lisowski, M., Major, J.J., Malone, S.D., Messerich, J.A., Moran, S.C., Pallister, J.S., Qamar, A.I., Schilling, S.P., and Vallance, J.W., 2006, Dynamics of seismogenic volcanic extrusion at Mount St. Helens in 2004–05: Nature, v. 444, no. 7118, p. 439–443, doi:10.1038/nature05322.

Jonientz-Trisler, C., Myers, B., and Power, J.A., 1994, Seismic identification of gas-and-ash explosions at Mount St. Helens—capabilities, limitations, and regional applications, *in* Casadevall, T.J., ed., Volcanic ash and aviation safety; proceedings of the First International Symposium on Volcanic Ash and Aviation Safety: U.S. Geological Survey Bulletin 2047, p. 351–356.

Lahr, J.C., Chouet, B.A., Stephens, C.D., Power, J.A., and Page, R.A., 1994, Earthquake classification, location, and error analysis in a volcanic environment; implications for the magmatic system of the 1989–1990 eruptions at Redoubt Volcano, Alaska: Journal of Volcanology and Geothermal Research, v. 62, nos. 1–4, p. 137–151, doi:10.1016/0377-0273(94)90031-0.

Lees, J.M., 1992, The magma system of Mount St. Helens: non-linear high-resolution P-wave tomography: Journal of Volcanology and Geothermal Research, v. 53, nos. 1–4, p. 103–116.

Lees, J.M., and Crosson, R.S., 1989, Tomographic inversion

for three-dimensional velocity structure at Mount St. Helens using earthquake data: Journal of Geophysical Research, v. 94, p. 5716–5728.

MacCarthy, J.K., and Rowe, C.A., 2005, Automatic scanning detection for characterization of dome-related seismic swarms at Mount St. Helens and their evolution through time [abs]: Eos (American Geophysical Union Transactions), v. 86, Fall Meeting Supplement, V53D-1591.

Major, J.J., Kingsbury, C.G., Poland, M.P., and LaHusen, R.G., 2008, Extrusion rate of the Mount St. Helens lava dome estimated from terrestrial imagery, November 2004–December 2005, chap. 12 *of* Sherrod, D.R., Scott, W.E., and Stauffer, P.H., eds., A volcano rekindled; the renewed eruption of Mount St. Helens, 2004–2006: U.S. Geological Survey Professional Paper 1750 (this volume).

Malone, S.D., 1983, Volcanic earthquakes; examples from Mount St. Helens, *in* Earthquakes—observations, theory and interpretation: Bologna, Italy, Società Italiana di Fisica, p. 436–455.

Malone, S.D., Endo, E.T., Weaver, C.S., and Ramey, J.W., 1981, Seismic monitoring for eruption prediction, *in* Lipman, P.W., and Mullineaux, D.R., eds., The 1980 eruptions of Mount St. Helens, Washington: U.S. Geological Survey Professional Paper 1250, p. 803–813.

Malone, S.D., Boyko, C., and Weaver, C.S., 1983, Seismic precursors to the Mount St. Helens eruptions in 1981 and 1982: Science, v. 221, p. 1376–1378.

Mastin, L.G., 1994, Explosive tephra emissions at Mount St. Helens, 1989–1991; the violent escape of magmatic gas following storms?: Geological Society of America Bulletin, v. 106, no. 2, p. 175–185.

Mastin, L.G., Roeloffs, E., Beeler, N.M., and Quick, J.E., 2008, Constraints on the size, overpressure, and volatile content of the Mount St. Helens magma system from geodetic and dome-growth measurements during the 2004–2006+ eruption, chap. 22 *of* Sherrod, D.R., Scott, W.E., and Stauffer, P.H., eds., A volcano rekindled; the renewed eruption of Mount St. Helens, 2004–2006: U.S. Geological Survey Professional Paper 1750 (this volume).

Matoza, R.S., Hedlin, M.A.H., and Garcés, M.A., 2007, An infrasound array study of Mount St. Helens: Journal of Volcanology and Geothermal Research, v. 160, p. 249–262, doi:10.1016/j.jvolgeores.2006.10.006.

McChesney, P.J., Couchman, M.R., Moran, S.C., Lockhart, A.B., Swinford, K.J., and LaHusen, R.G., 2008, Seismic-monitoring changes and the remote deployment of seismic stations (seismic spider) at Mount St. Helens, 2004–2005, chap. 7 *of* Sherrod, D.R., Scott, W.E., and Stauffer, P.H., eds., A volcano rekindled; the renewed eruption of Mount St. Helens, 2004–2006: U.S. Geological Survey Professional Paper 1750 (this volume).

Mogi, K., 1962, Magnitude-frequency relation for elastic shocks accompanying fractures of various materials and some related problems in earthquakes: Bulletin of the Earthquake Research Institute, v. 40, p. 831–853.

Moran, S.C., 1994, Seismicity at Mount St. Helens, 1987–1992; evidence for repressurization of an active magmatic system: Journal of Geophysical Research, v. 99, no. B3, p. 4341–4354, doi:10.1029/93JB02993.

Moran, S.C., and Malone, S.D., 2004, Seismicity associated with the first month of the 2004 eruption of Mount St. Helens [abs]: Eos (American Geophysical Union Transactions), v. 85, Fall Meeting Supplement, V31E-02.

Moran, S.C., Lees, J.M., and Malone, S.D., 1999, P-wave crustal velocity structure in the greater Mount Rainier area from local earthquake tomography: Journal of Geophysical Research, v. 104, p. 10775–10786.

Moran, S.C., McChesney, P.J., and Lockhart, A.B., 2008, Seismicity and infrasound associated with explosions at Mount St. Helens, 2004–2005, chap. 6 *of* Sherrod, D.R., Scott, W.E., and Stauffer, P.H., eds., A volcano rekindled; the renewed eruption of Mount St. Helens, 2004–2006: U.S. Geological Survey Professional Paper 1750 (this volume).

Musumeci, C., Gresta, S., and Malone, S.D., 2002, Magma system recharge of Mount St. Helens from precise relative hypocenter location of microearthquakes: Journal of Geophysical Research, v. 107, no. B10, 2264, p. ESE 16-1–ESE 16-9, doi:10.1029/2001JB000629.

Neuberg, J.W., Tuffen, H., Collier, L., Green, D., Powell, T., and Dingwell, D., 2006, The trigger mechanism of low-frequency earthquakes on Montserrat: Journal of Volcanology and Geothermal Research, v. 153, nos. 1–2, p. 37–50, doi:10.1016/j.jvolgeores.2005.08.00.

Norris, R.D., 1994, Seismicity of rockfalls and avalanches at three Cascade Range volcanoes; implications for seismic detection of hazardous mass movements: Bulletin of the Seismological Society of America, v. 84, p. 1925–1939.

Okada, H., Watanabe, H. Yamashita, H., and Yokoyama, I., 1981, Seismological significance of the 1977–1978 eruptions and the magma intrusion process of Usu Volcano, Hokkaido: Journal of Volcanology and Geothermal Research, v. 9, p. 311–334.

Pallister, J.S., Hoblitt, R.P., Crandell, D.R., and Mullineaux, D.R., 1992, Mount St. Helens a decade after the 1980 eruptions; magmatic models, chemical cycles, and a revised hazards assessment: Bulletin of Volcanology, v. 54, no. 2, p. 126–146, doi: 10.1007/BF00278003.

Poland, M.P., and Lu, Z., 2008, Radar interferometry observations of surface displacements during pre- and coeruptive

periods at Mount St. Helens, Washington, 1992–2005, chap. 18 *of* Sherrod, D.R., Scott, W.E., and Stauffer, P.H., eds., A volcano rekindled; the renewed eruption of Mount St. Helens, 2004–2006: U.S. Geological Survey Professional Paper 1750 (this volume).

Power, J.A., 1988, Seismicity associated with the 1986 eruption of Augustine Volcano, Alaska: Fairbanks, University of Alaska, M.S. thesis, 142 p.

Power, J.A., Lahr, J.C., Page, R.A., Chouet, B.A., Stephens, C.D., Harlow, D.H., Murray, T.L., and Davies, J.N., 1994, Seismic evolution of the 1989–1990 eruption sequence of Redoubt Volcano, Alaska: Journal of Volcanology and Geothermal Research, v. 62, p. 69–94.

Qamar, A.I., St. Lawrence, W., Moore, J.N., and Kendrick, G., 1983, Seismic signals preceding the explosive eruption of Mount St. Helens, Washington, on 18 May 1980: Bulletin of the Seismological Society of America, v. 73, p. 1797–1813.

Qamar, A.I., Malone, S.D., Moran, S.C., Steele, W.P., and Thelen, W.A., 2008, Near-real-time information products for Mount St. Helens—tracking the ongoing eruption, chap. 3 *of* Sherrod, D.R., Scott, W.E., and Stauffer, P.H., eds., A volcano rekindled; the renewed eruption of Mount St. Helens, 2004–2006: U.S. Geological Survey Professional Paper 1750 (this volume).

Reasenberg, P.A., and Oppenheimer, D., 1985, FPFIT, FPPLOT, and FPPAGE: FORTRAN computer programs for calculating and plotting earthquake fault-plane solutions: U.S. Geological Survey Open-File Report 85–739, 109 p.

Rowe, C.A., Thurber, C.H., and White, R.A., 2004, Dome growth behavior at Soufriere Hills Volcano, Montserrat, revealed by relocation of volcanic event swarms, 1995–1996: Journal of Volcanology and Geothermal Research, v. 134, no. 3, p. 199–221.

Scandone, R., and Malone, S.D., 1985, Magma supply, magma discharge, and readjustment of the feeding system of Mount St. Helens during 1980: Journal of Volcanology and Geothermal Research, v. 23, nos. 3–4, p. 239–262, doi:10.1016/0377-0273(85)90036-8.

Schilling, S.P., Thompson, R.A., Messerich, J.A., and Iwatsubo, E.Y., 2008, Use of digital aerophotogrammetry to determine rates of lava dome growth, Mount St. Helens, Washington, 2004–2005, chap. 8 *of* Sherrod, D.R., Scott, W.E., and Stauffer, P.H., eds., A volcano rekindled; the renewed eruption of Mount St. Helens, 2004–2006: U.S. Geological Survey Professional Paper 1750 (this volume).

Schneider, D.J., Vallance, J.W., Wessels, R.L., Logan, M., and Ramsey, M.S., 2008, Use of thermal infrared imaging for monitoring renewed dome growth at Mount St. Helens, 2004, chap. 17 *of* Sherrod, D.R., Scott, W.E., and Stauffer, P.H., eds., A volcano rekindled; the renewed eruption of Mount St. Helens, 2004–2006: U.S. Geological Survey Professional Paper 1750 (this volume).

Scott, W.E., Sherrod, D.R., and Gardner, C.A., 2008, Overview of the 2004 to 2006, and continuing, eruption of Mount St. Helens, Washington, chap. 1 *of* Sherrod, D.R., Scott, W.E., and Stauffer, P.H., eds., A volcano rekindled; the renewed eruption of Mount St. Helens, 2004–2006: U.S. Geological Survey Professional Paper 1750 (this volume).

Shemeta, J., and Weaver, C.S., 1986, Seismicity accompanying the May 18, 1980, eruption of Mount St. Helens, Washington, *in* Keller, S.A.C., ed., Mount St. Helens, five years later: Cheney, Wash., Eastern Washington University Press, p. 44–58.

Swanson, D.A., and Holcomb, R.T., 1990, Regularities in growth of the Mount St. Helens dacite dome, 1980–1986, *in* Fink, J.H., ed., Lava flows and domes, emplacement mechanisms and hazard implications: Berlin, Springer-Verlag, International Association of Volcanology and Chemistry of the Earth's Interior, Proceedings in Volcanology 2, p. 3–24.

Swanson, D.A., Casadevall, T.J., Dzurisin, D., Malone, S.D., Newhall, C.G., and Weaver, C.S., 1983, Predicting eruptions at Mount St. Helens, June 1980 through December 1982: Science, v. 221, no. 4618, p. 1369–1376.

Swanson, D.A., Casadevall, T.J., Dzurisin, D., Malone, S.D., Holcomb, R.T., Newhall, C.G., and Weaver, C.S., 1985, Forecasts and predictions of eruptive activity at Mount St. Helens, USA; 1975–1984: Journal of Geodynamics, v. 3, p. 397–423.

Thelen, W.A., Crosson, R.S., and Creager, K.C., 2008, Absolute and relative locations of earthquakes at Mount St. Helens, Washington, using continuous data; implications for magmatic processes, chap. 4 *of* Sherrod, D.R., Scott, W.E., and Stauffer, P.H., eds., A volcano rekindled; the renewed eruption of Mount St. Helens, 2004–2006: U.S. Geological Survey Professional Paper 1750 (this volume).

Vallance, J.W., Schneider, D.J., and Schilling, S.P., 2008, Growth of the 2004–2006 lava-dome complex at Mount St. Helens, Washington, chap. 9 *of* Sherrod, D.R., Scott, W.E., and Stauffer, P.H., eds., A volcano rekindled; the renewed eruption of Mount St. Helens, 2004–2006: U.S. Geological Survey Professional Paper 1750 (this volume).

Villagómez, D., 2000, Sismícidad del volcán Guagua Pichincha 1998–1999: Quito, Ecuador, Escuela Politécnica Nacional, M.S. thesis.

Vinciguerra, S., Gresta, S., Barbano, M.S., and Distefano, G., 2001, The two behaviours of Mt. Etna Volcano before and after a large intrusive episode; evidences from *b* value and fractal dimension of seismicity: Geophysical Research Letters, v. 28, p. 2257–2260.

Waite, G.P., Chouet, B.A. and Dawson, P.B., 2008, Eruption dynamics at Mount St. Helens imaged from broadband seismic waveforms; interaction of the shallow magmatic and hydrothermal systems: Journal of Geophysical Research, v. 113, B02305, 22 p., doi:10.1029/2007JB005259.

Walder, J.S., Schilling, S.P., Vallance, J.W., and LaHusen, R.G., 2008, Effects of lava-dome growth on the Crater Glacier of Mount St. Helens, Washington, chap. 13 *of* Sherrod, D.R., Scott, W.E., and Stauffer, P.H., eds., A volcano rekindled; the renewed eruption of Mount St. Helens, 2004–2006: U.S. Geological Survey Professional Paper 1750 (this volume).

Weaver, C.S., Grant, W.G., Malone, S.D., and Endo, E.T., 1981, Post-May 18 seismicity; volcanic and tectonic implications, *in* Lipman, P.W., and Mullineaux, D.R., eds., The 1980 eruptions of Mount St. Helens, Washington: U.S. Geological Survey Professional Paper 1250, p. 109–121.

Weaver, C.S., Zollweg, J.E., and Malone, S.D., 1983, Deep earthquakes beneath Mount St. Helens; evidence for magmatic gas transport?: Science, v. 221, p. 1391–1394.

Weaver, C.S., Grant, W.C., and Shemeta, J.E., 1987, Local crustal extension at Mount St. Helens, Washington: Journal of Geophysical Research, v. 92, no. B10, p. 10170–10178.

Wiemer, S., and McNutt, S.R., 1997, Variations in the frequency-magnitude distribution with depth in two volcanic areas—Mount St. Helens, Washington, and Mt. Spurr, Alaska: Geophysical Research Letters, v. 24, p. 189–192.

# Appendix 1. PNSN Fault-Plane Solutions, 09/23/04–12/31/05

This appendix comprises numerous plots showing first motions and preferred fault-plane solutions for well-constrained events (maximum azimuthal gap <135°, nearest station <1 km, and at least 10 picked phase arrivals) (fig. 25) in the PNSN catalog from September 24 to November 27, 2004, and for "big" events from November 27, 2004 to December 31, 2005 (fig. 26). We did not review fault-plane solutions from the PNSN catalog except those for the "big" events. Only those fault-plane solutions with at least 10 polarities are shown. Note that all fault-plane solution times are in Coordinated Universal Time (UTC), in contrast to the local time convention used in the rest of this paper. All fault-plane solutions were determined using the FPFIT computer program (Reasenberg and Oppenheimer, 1985).

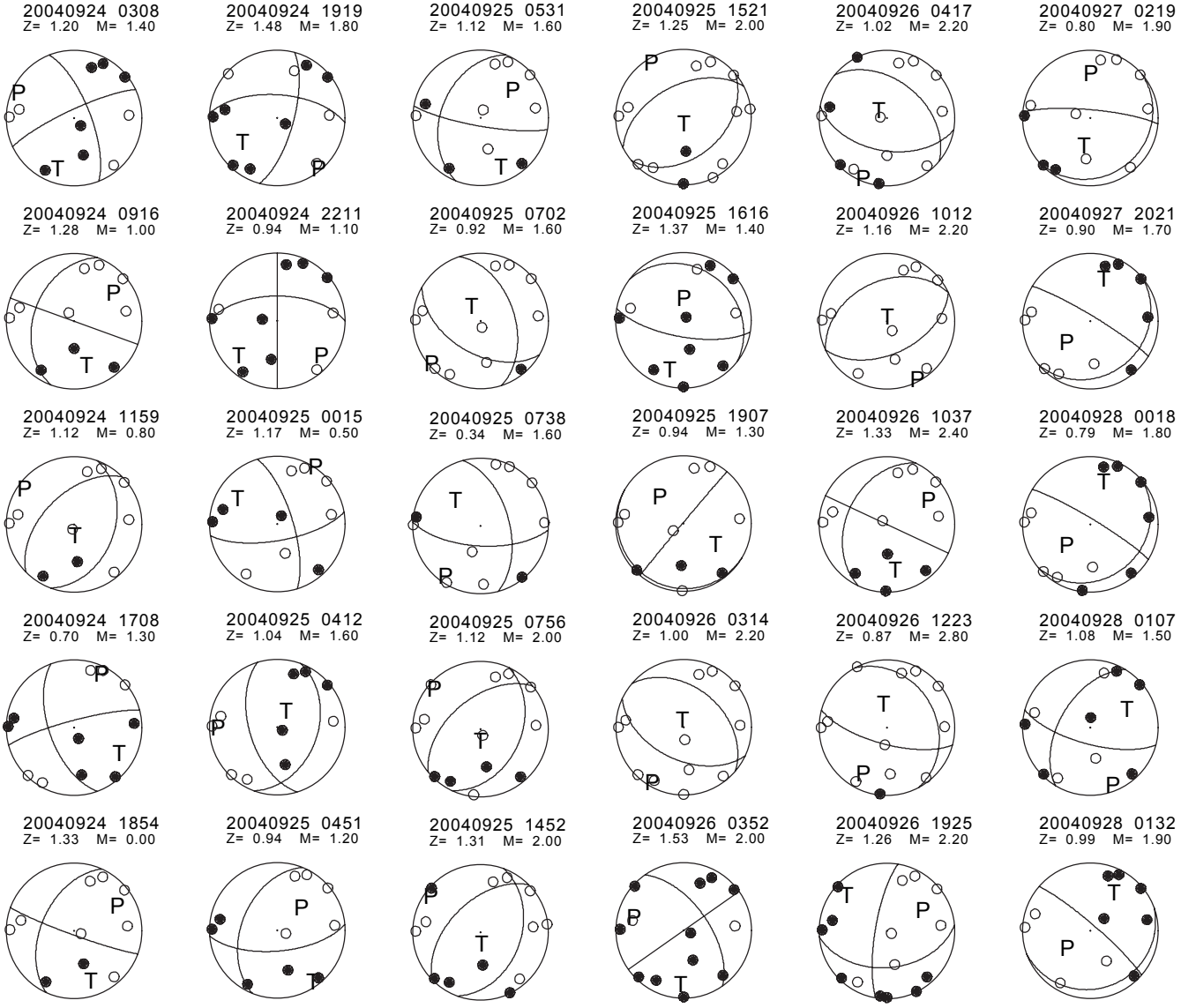


**Figure 25.** Fault-plane solutions for 161 earthquakes occurring at Mount St. Helens during the period from Sept. 24 to Oct. 11, 2004. P, compressional axis; T, tensional axis. Open circles correspond to dilatational (down) first motions, closed circles to compressional (up) first motions. Each solution is coded for date and time (UTC) in this format: YYYYMMDD hhmm. Z, depth, in kilometers; M, magnitude.

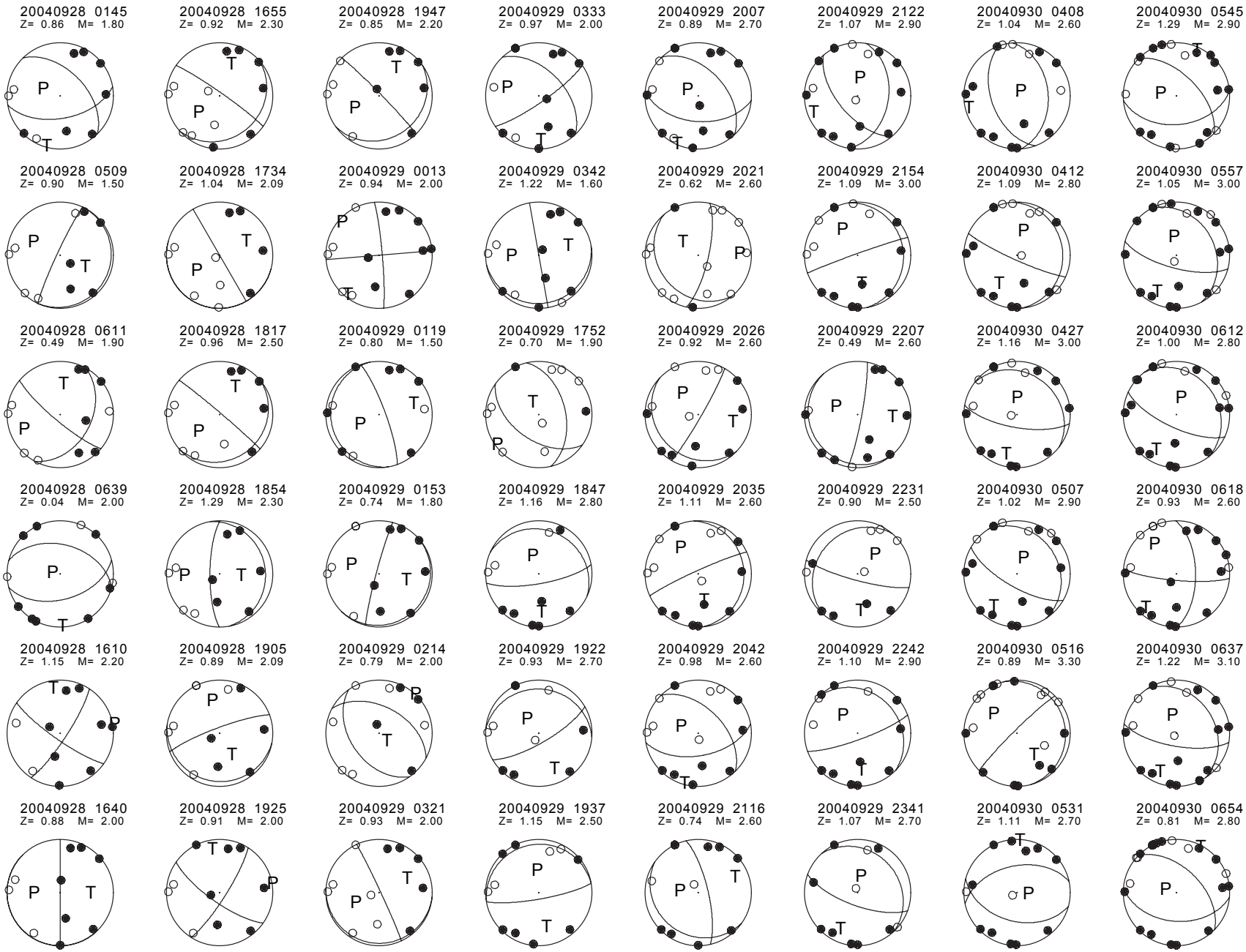


**Figure 25—Continued.**

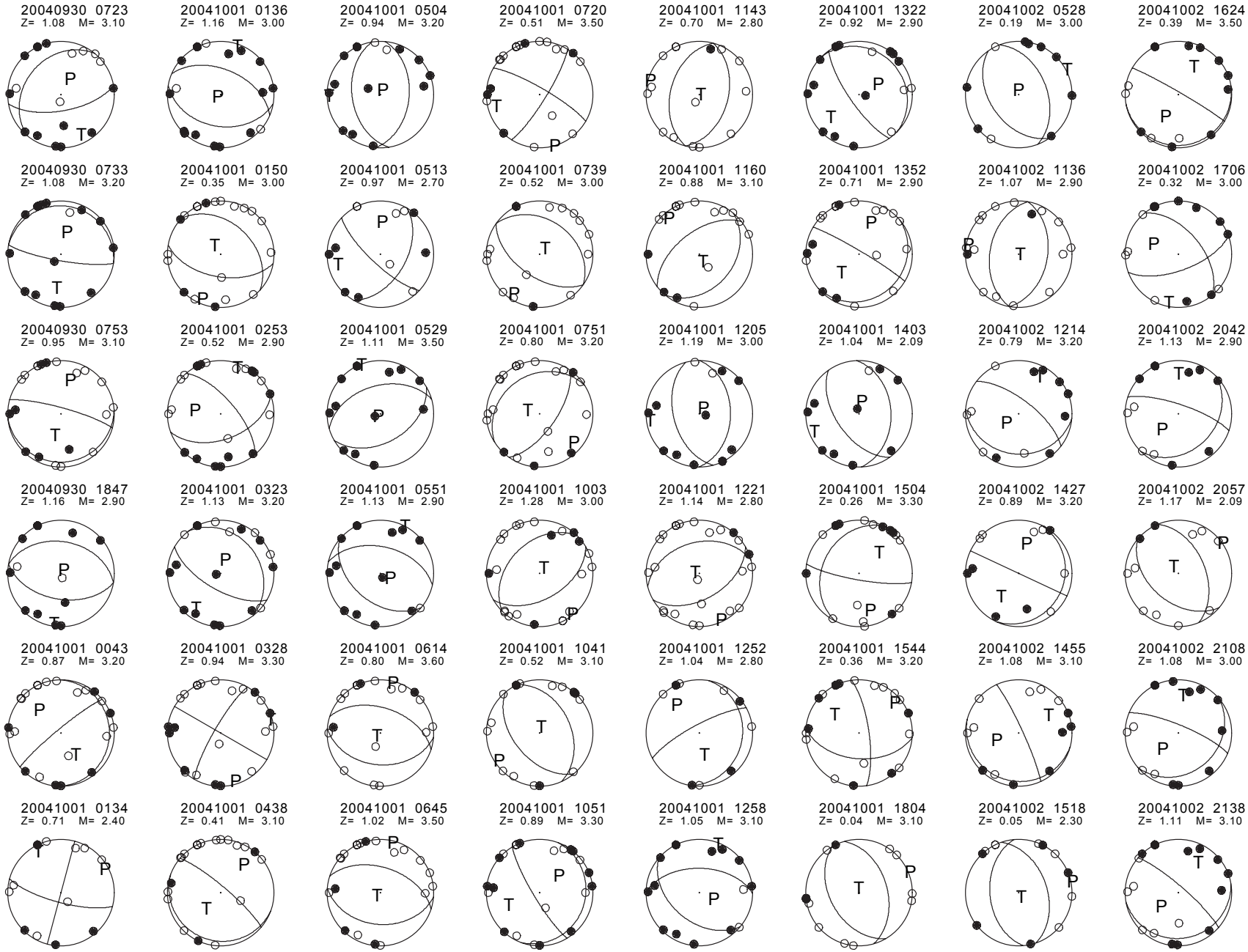


**Figure 25—Continued.**

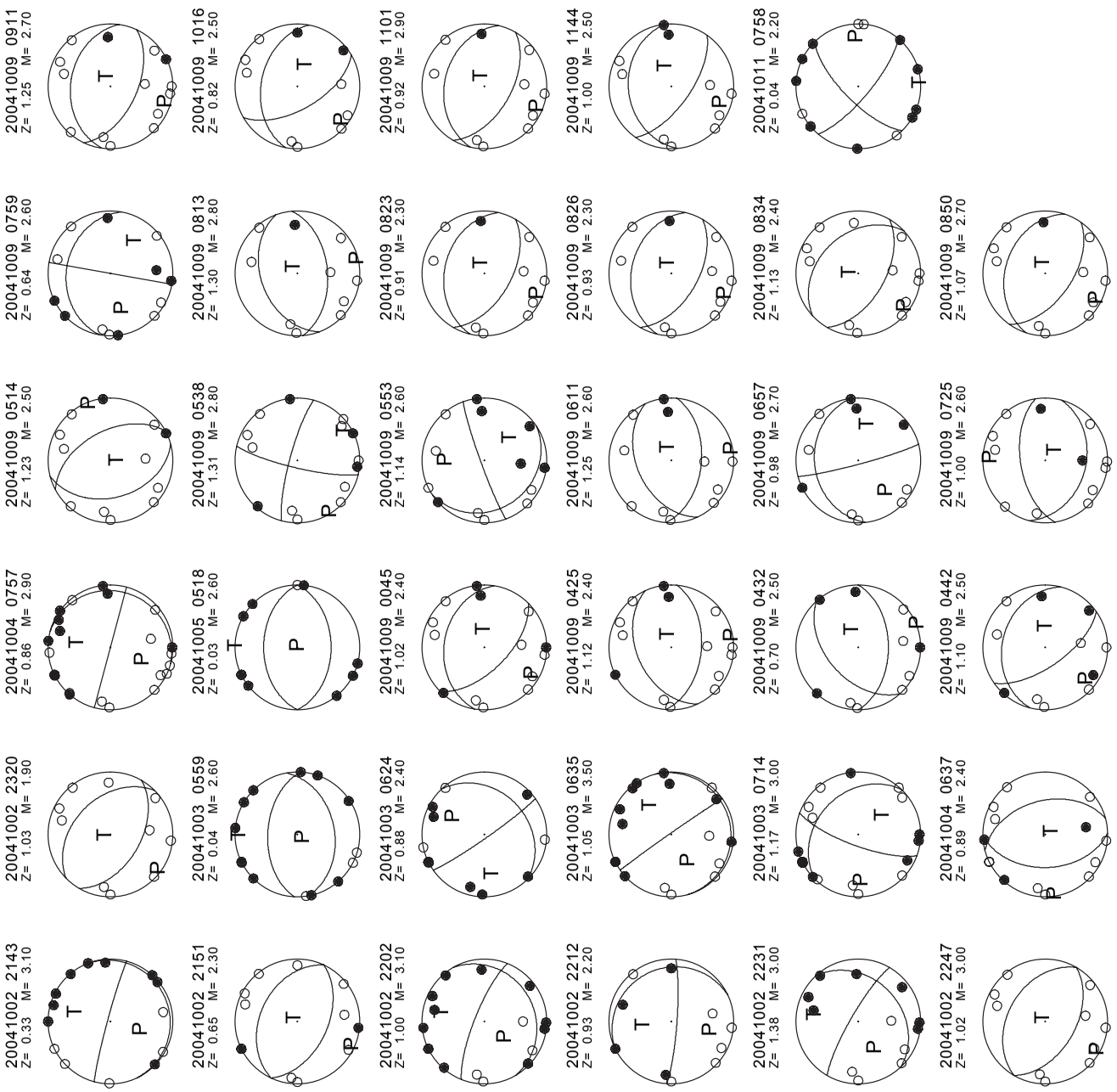


**Figure 25—Continued.**

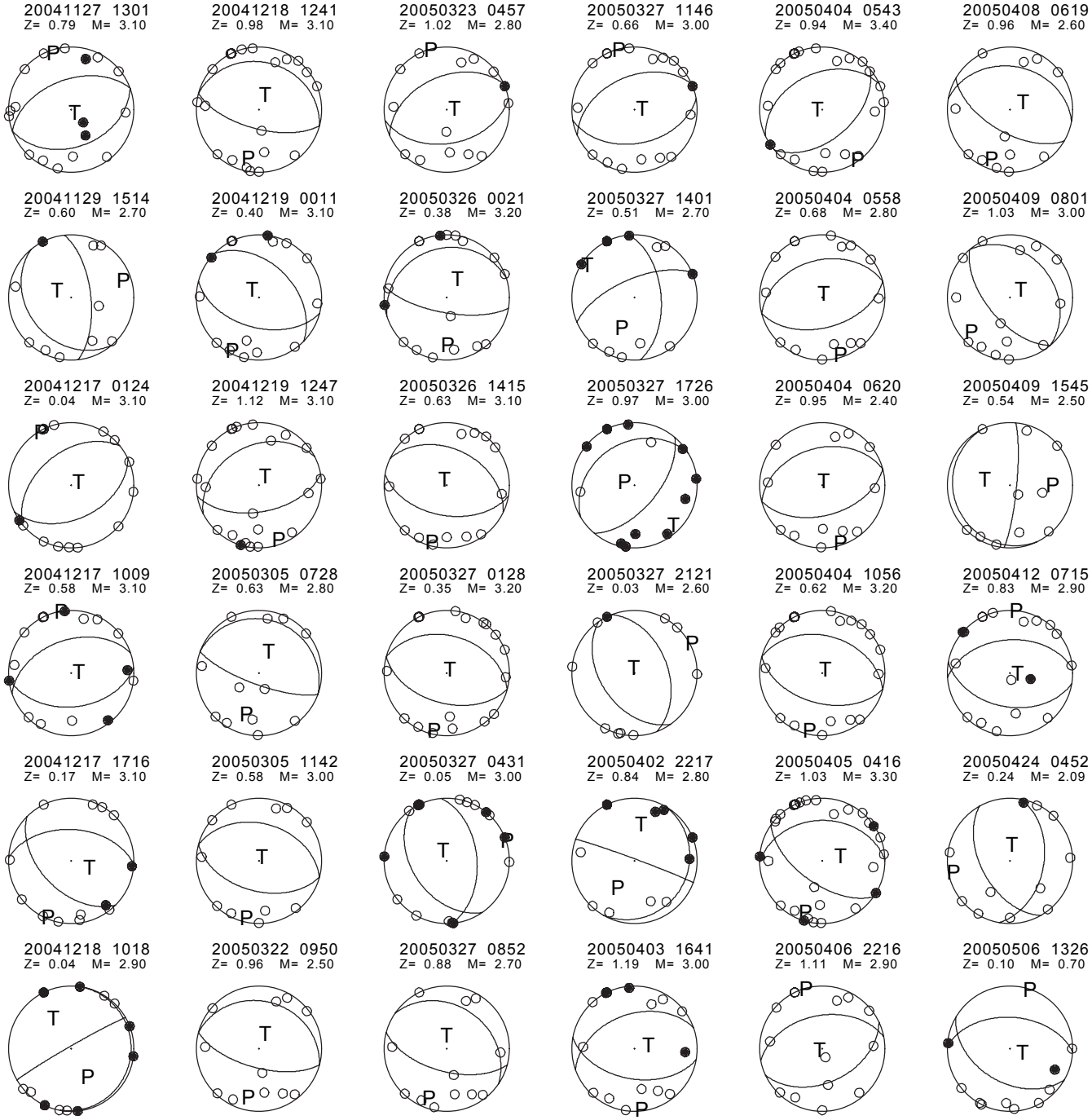


**Figure 26.** Fault-plane solutions for 55 earthquakes ($M_d$ 0.7–3.4) occurring at Mount St. Helens during the period from Nov. 27, 2004, to Oct. 7, 2005. P, compressional axis; T, tensional axis. Open circles correspond to dilatational (down) first motions, closed circles to compressional (up) first motions. Each solution is coded for date and time (UTC) in this format: YYYYMMDD hhmm. Z, depth, in kilometers; M, magnitude.

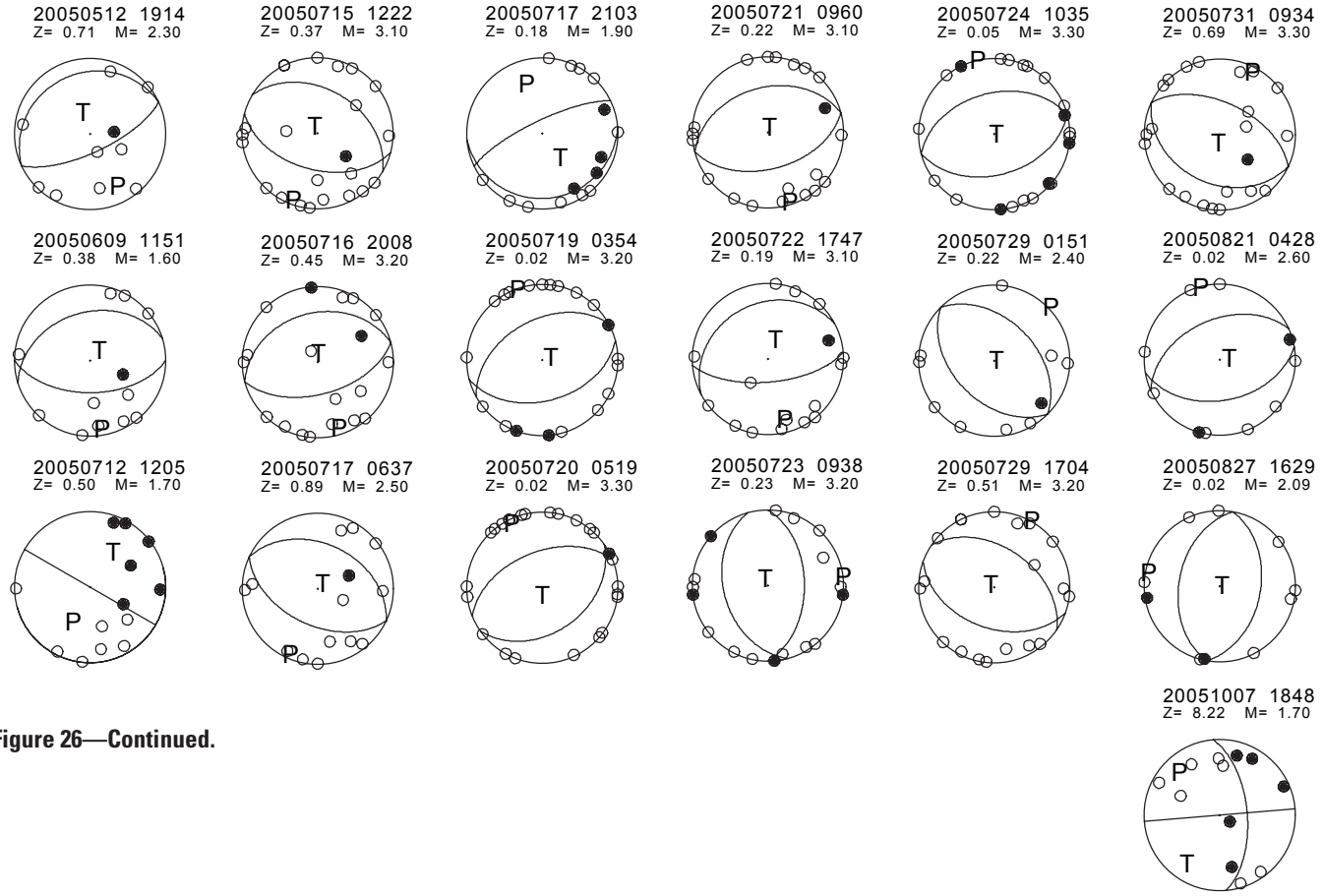


**Figure 26—Continued.**

# Appendix 2. Automated Event Detection

Analyst-driven earthquake location quickly became infeasible as a means for tracking the course of the eruption because it was too slow (Qamar and others, this volume, chap. 3), so over subsequent months we developed methods for automatically detecting events and recording several event parameters of interest. Figures 5, 13, and 14 show results from one such method, a standard triggering algorithm that uses the ratio of average seismic amplitudes computed over short- and long-term time windows, as applied to station HSR (fig. 1). We chose HSR over other stations for three principal reasons: (1) it is a sensitive site that usually records even small earthquakes cleanly; (2) wind noise is usually insignificant; and (3) after a gain reduction on October 4, 2004, no changes were made to the site (McChesney and others, this volume, chap. 7). We used averaging windows of 1 s and 8 s for the short- and long-term averages and a triggering ratio of 2.3 that was determined to be optimal for HSR through trial and error. To avoid multiple triggers from the same event, we skipped forward 6 s after each trigger. We also devised station-specific algorithms for distinguishing between noise glitches (including telemetry and/or Internet dropouts, radio interference, and calibration pulses) and events, although some glitches still made it through our filters. To test the impact of such noise-induced event detections, we visually scanned through helicorder plots for selected time periods and removed glitches that had been recorded as events. Although the resulting plots were cleaner, the fundamental trends were unchanged; in essence, noise was overwhelmed by the shear number of earthquakes.

For each detected event we recorded the peak amplitude over the next 6 s (usually the S wave at HSR), the time gap between successive events, and the normalized power spectra for the first 256 samples following the P-wave arrival (or 2.56 s with the 100-Hz sample rate used by the PNSN and CVO for all short-period stations). We chose to look only at spectra for the first 2.56 s (256 samples) following the event trigger, as full-event spectra were dominated by surface-wave energy and were thus not useful in detecting subtle changes in source spectra, particularly between hybrid and LF events. We only show spectra for events with amplitudes greater than 300 counts ($M_d$ ~1.0), because our algorithm commonly triggered on the S-wave for events smaller than this threshold. The resulting spectra plots, which we referred to as ESAM (Earthquake Spectral AMplitude) plots, proved to be more useful for assessing changes in earthquake source frequency than standard spectrograms of continuous seismic data, particularly because eruption-related seismicity was dominated by discrete seismic events.